

Stratigraphic evolution of an outcropping continental slope system, Tres Pasos Formation at Cerro Divisadero, Chile

BRIAN W. ROMANS^{*·1}, STEPHEN M. HUBBARD[†] and STEPHAN A. GRAHAM^{*}

^{*}*Dept. of Geological & Environmental Sciences, Stanford University, 450 Serra Mall, Bldg 320, Stanford, CA 94305, USA (E-mail: brian.romans@chevron.com)*

[†]*Dept. of Geoscience, University of Calgary, 2500 University Drive NW, Calgary, AB, T2N 1N4 Canada*

Associate Editor: Ole Martinsen

ABSTRACT

Depositional slope systems along continental margins contain a record of sediment transfer from shallow-water to deep-water environments and represent an important area for natural resource exploration. However, well-preserved outcrops of large-scale depositional slopes with seismic-scale exposures and tectonically intact stratigraphy are uncommon. Outcrop characterization of smaller-scale depositional slope systems (i.e. <700 m of undecompressed shelf-to-basin relief) has led to increased understanding of stratigraphic packaging of prograding slopes. Detailed stacking patterns of facies and sedimentary body architecture for larger-scale slope systems, however, remain understudied. The Cretaceous Tres Pasos Formation of the Magallanes Basin, southern Chile, presents a unique opportunity to evaluate the stratigraphic evolution of such a slope system from an outcrop perspective. Inherited tectonic relief from a precursor oceanic basin phase created shelf-to-basin bathymetry comparable with continental margin systems (~1000 m). Sedimentological and architectural data from the Tres Pasos Formation at Cerro Divisadero reveal a record of continental margin-scale depositional slope progradation and aggradation. Slope progradation is manifested as a vertical pattern exhibiting increasing amounts of sediment bypass upwards, which is interpreted as reflecting increasing gradient conditions. The well-exposed, seismic-scale outcrop is characterized by four 20 to 70 m thick sandstone-rich successions, separated by mudstone-rich intervals of comparable thickness (40 to 90 m). Sedimentary body geometry, facies distribution, internal bedding architecture, sandstone richness and degree of amalgamation were analysed in detail across a continuous 2.5 km long transect parallel to depositional dip. Deposition in the lower section (Units 1 and 2) was dominated by poorly channelized to unconfined sand-laden flows and accumulation of mud-rich mass transport deposits, which is interpreted as representing a base of slope to lower slope setting. Evidence for channelization and indicators of bypass of coarse-grained turbidity currents are more common in the upper part of the >600 m thick succession (Units 3 and 4), which is interpreted as reflecting increased gradient conditions as the system accreted basinward.

Keywords Deep-water stratigraphy, foreland basin, Magallanes Basin, progradation, slope deposits, turbidite architecture, turbidite processes.

¹Present address: Chevron Energy Technology Company, 6001 Bollinger Canyon Rd., San Ramon, CA 94583, USA.

INTRODUCTION

Depositional slopes connect deep-marine basins to their coeval shallow-water delivery systems. The deposits of this important depositional environment record evidence of sediment supply, creation and destruction of accommodation, and tectonic processes (Flint & Hodgson, 2005). Understanding the stratigraphic packaging of large-scale prograding shelf-slope systems is fundamental to understanding how sedimentary basins fill and the evolution of supply-dominated continental margins.

Studies utilizing seismic reflection and/or bathymetric data have documented clinofold and clinofold geometries in continental slope systems (e.g. Winker & Edwards, 1983; Fulthorpe & Austin, 1998; Pirmez *et al.*, 1998; Driscoll & Karner, 1999) but few studies have documented detailed facies relationships and sedimentary body geometries of slope deposits at higher resolutions. Outcrops provide an opportunity for such high-resolution investigation; however, the preservation of extensive, and stratigraphically intact, continental-margin slope systems is extremely rare. Detailed outcrop studies of depositional slopes over the past decade have focused on relatively small systems that developed in basins on continental crust with relatively shallow water depths (e.g. Eocene strata of Spitsbergen, Plink-Björklund & Steel, 2005). The present study focuses on an exceptionally well-exposed Cretaceous slope succession in the Magallanes foreland basin of southern South America. Slope strata of the Tres Pasos Formation at Cerro Divisadero prograded into a relatively deep retroarc foreland basin that developed on attenuated crust. The aim of this study was to document and interpret the stacking patterns and stratigraphic evolution of a large-scale depositional slope system based on sedimentological and architectural examination of turbidite bodies.

TECTONIC SETTING

The Tres Pasos Formation is the uppermost of three turbiditic formations that make up the bulk of the Magallanes foreland basin fill (>4000 m thick; Fig. 1). The Magallanes Basin is located along the south-western margin of the South American plate, east of the Andes volcanic arc (Fig. 2). Closure of a precursor back-arc basin (Rocas Verdes Basin) in the Early Cretaceous corresponded with development of the eastward-vergent Andean fold-thrust

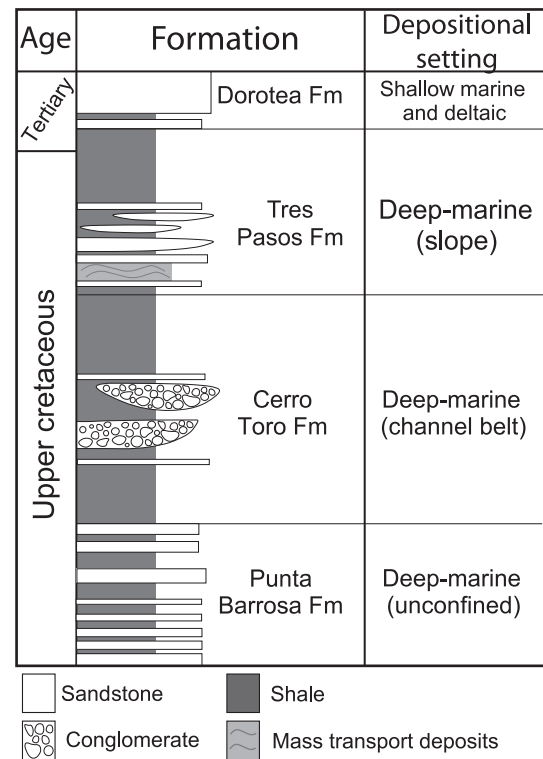


Fig. 1. Generalized stratigraphic column for outcropping Magallanes foreland basin strata in the Patagonian Andes of southern Chile. Outcrops of slope deposits in the lower part of the Tres Pasos Formation are the focus of this study.

belt (Dalziel *et al.*, 1974; Wilson, 1991). Deep-marine sedimentation initiated in the early Magallanes foreland basin (Punta Barrosa Formation) was related to loading by obducted oceanic crust (Sarmiento Ophiolite), which caused flexural subsidence in the retroarc position (Dalziel, 1986; Wilson, 1991; Fildani & Hessler, 2005) (Fig. 1). Continued and persistent subsidence, coupled with high sediment supply as a result of denudation of an active arc and fold-thrust belt during the Late Cretaceous, is recorded by the deep-water conglomeratic Cerro Toro Formation and overlying slope system of the Tres Pasos Formation (Fig. 1; Katz, 1963; Scott, 1966; Natland *et al.*, 1974; Biddle *et al.*, 1986; Wilson, 1991; Fildani & Hessler, 2005). Palaeocurrent data from the Punta Barrosa, Cerro Toro and Tres Pasos formations indicate consistent north-to-south sediment dispersal (i.e. parallel to trend of fold-thrust belt), reflecting foreland subsidence patterns (Scott, 1966; Winn & Dott, 1979; Fildani & Hessler, 2005; Shultz *et al.*, 2005; Hubbard *et al.*, 2008). Eastward migration of the fold-thrust belt continued into the Tertiary, uplifting the deep-water strata into its present position (Fig. 2).

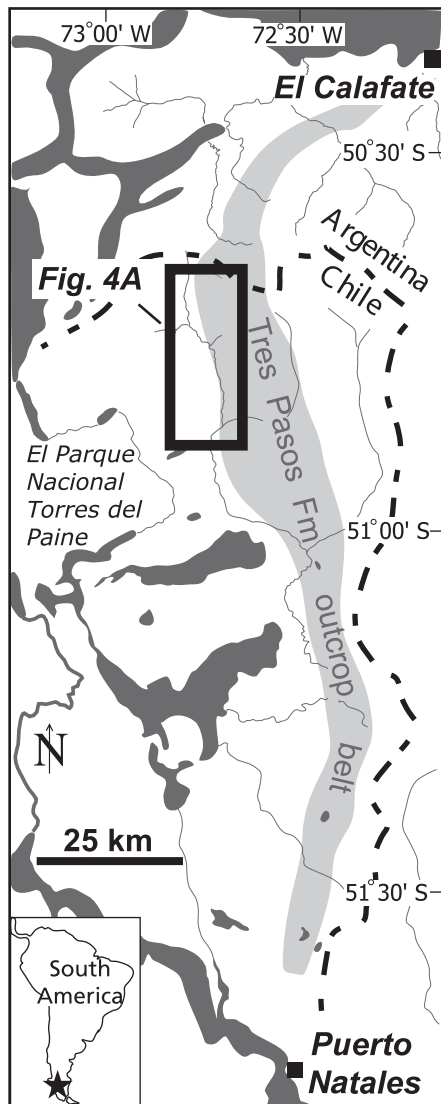


Fig. 2. Regional geography of the Ultima Esperanza District of southern Chile and El Calafate area of Argentina. Upper Cretaceous strata crop out in a north-south belt in the foothills east of the Patagonian Andes. Area shaded in light grey refers to Tres Pasos Formation outcrop belt. Average palaeocurrents are north-to-south, generally parallel to outcrop belt. See Fig. 3 for regional dip-oriented stratigraphic framework. Box refers to location of Cerro Divisadero outcrop location shown in Fig. 4A.

PALAEOGEOGRAPHIC CONTEXT AND PREVIOUS WORK

The Tres Pasos Formation consists of deposits of a delta-fed slope that prograded southward into the axial foreland basin during the latest Cretaceous (Fig. 3; Smith, 1977; Arbe & Hechem, 1985; Macellari *et al.*, 1989; Shultz *et al.*, 2005). Although the basin-scale pattern of southward

progradation has been recognized (Fig. 3; Arbe & Hechem, 1985; Macellari *et al.*, 1989), detailed stratigraphic relationships remain poorly understood. Shultz *et al.* (2005) documented the general character of facies and sedimentary body architecture for the Tres Pasos Formation at multiple locations along a 70 km long outcrop belt (Figs 2 and 3). The present study focuses on the most proximal location characterized by thick sandstone-rich intervals in the Tres Pasos belt. Exposures ~15 km to the north (i.e. landward) in Argentina are almost exclusively shale, with rare thin sandy turbidites. Further north, ~30 km from the study area, slope deposits are replaced completely by shallow-marine strata (Fig. 3; Arbe & Hechem, 1985; Macellari *et al.*, 1989). The Chile–Argentina border is thus roughly coincident with a regional facies boundary between dominantly shallow-water strata to the north and deep-water strata to the south (Figs 1 and 3). The northern limit of Upper Jurassic oceanic crust, remnants of the predecessor back-arc basin, is near this latitude, suggesting an underlying tectonic control on the regional depositional profile during the Cretaceous (Biddle *et al.*, 1986; Wilson, 1991; Fildani & Hessler, 2005).

The transition from shale of the uppermost Cerro Toro Formation to mass transport deposits and lenticular sandstone-rich bodies of the Tres Pasos Formation marks the onset of slope sedimentation at this inherited bathymetric declivity. Although direct measures of palaeobathymetry are unavailable in the Tres Pasos Formation, the stratigraphic thickness from the uppermost Cerro Toro Formation, identified as bathyal water deposits (1000 to 2000 m) by Natland *et al.* (1974), to the shallow-marine deposits of the Dorotea Formation is as much as 1500 m (Figs 1 and 3). Water depths of at least several hundred metres are estimated conservatively for the lower Tres Pasos Formation and these depths could be significantly more if compaction is considered. The north–south transition from fully continental to quasi-oceanic crust is consistent with such bathymetric relief. This larger context permits further investigation of higher-resolution stratigraphic relationships related with geometry and extent of sandstone-rich clinotherm packages.

STUDY AREA

Sandstone-rich intervals of the Tres Pasos and overlying Dorotea formations are exposed for >100 km in the Ultima Esperanza District of

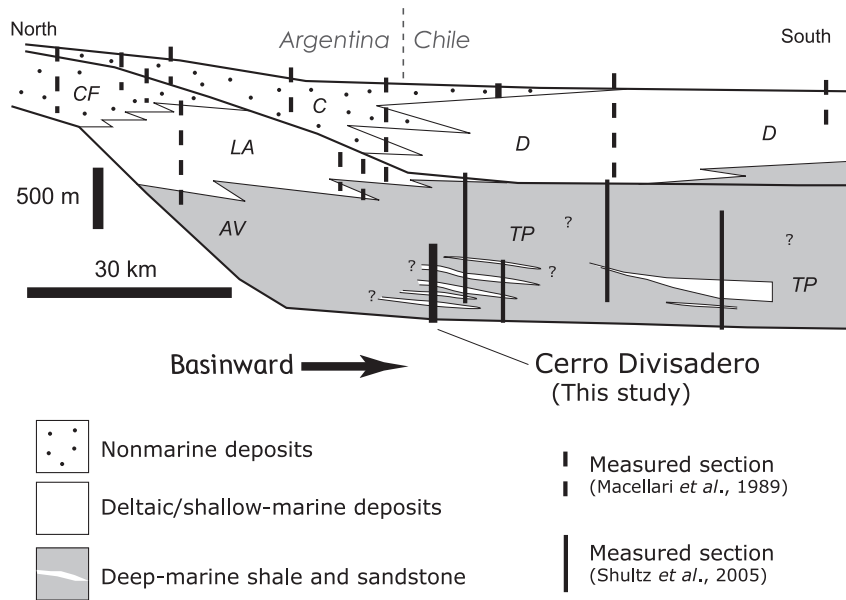


Fig. 3. Simplified regional stratigraphic framework for the Tres Pasos Formation slope system. Cross-section is modified from Macellari *et al.* (1989) with information from Shultz *et al.* (2005). This study is focused on the lower part of the Tres Pasos Formation at Cerro Divisadero. Formation names: CF, Cerro Fortoleza; LA, La Anita; C, Chorrillo; AV, Alta Vista; D, Dorotea; TP, Tres Pasos.

southern Chile in a series of east-dipping hogbacks that mark the eastern limit of the present southern Andean fold-thrust belt (Figs 2 and 3). Shultz *et al.* (2005) and Shultz & Hubbard (2005) documented general trends in facies and architecture at several Tres Pasos Formation outcrop locations in Ultima Esperanza. The present study focuses on Cerro Divisadero, the northernmost and least studied location of Shultz *et al.* (2005) (Figs 3 and 4). Over 600 m of stratigraphy is exposed in a continuous, 2.5 km long outcrop transect oriented sub-parallel to depositional dip in the southern part of this mountain (Fig. 4B and C). The studied succession, the lower part of the Tres Pasos Formation, comprises four sandstone-rich units ranging in thickness from 20 to 70 m. These four turbidite packages, herein termed 'Units 1 to 4' (from oldest to youngest), internally exhibit variable facies distribution and bedding architecture, lenticularity, sandstone richness, and degree of amalgamation. Shale-rich intervals of comparable (or slightly greater) thickness separate the sandstone-rich units (Fig. 4B and C). The thick (> 400 m) shale-dominated interval that overlies the studied succession is exposed on an extensive dip slope to the east of the main Cerro Divisadero ridgeline and is not assessed in this study (Fig. 4A). The gully and ridge topography of the west face of Cerro Divisadero creates local three-dimensionality, permitting investigation of relationships between stratal architecture and palaeocurrent information.

Post-depositional features present at Cerro Divisadero include minor reverse faults (and

associated folds) and local Tertiary intrusive and extrusive igneous rocks. The west-verging reverse faults probably are back-thrusts associated with the regional east-verging fold-thrust belt (Shultz *et al.*, 2005; after Wilson, 1991). Disruption of the overall stratigraphy is negligible (tens of metres of offset), although high-resolution architectural analysis is impacted negatively in some intervals. The igneous rocks, which are presumed to be related to regional magmatism during the Miocene (Halpern, 1973; Micael, 1983), are sparse and avoidable.

DATA AND APPROACH

Approximately 1800 m of detailed measured sections form the foundation of the data set. These sections capture characteristics at the scale of individual sedimentation units (centimetres to decimetres) including thickness, grain-size, sedimentary structures and nature of bedding contacts. Individual sedimentation units and their internal divisions represent fundamental depositional processes which are grouped into mappable facies (Table 1 and Fig. 5). Sections were tied together through physical correlation (i.e. walking out beds in the field) and photomosaic mapping. Characterization of sedimentary bodies and high-resolution stratal relationships help bridge the gap between facies analysis and formation-scale stratigraphy (Fig. 5). Sedimentary bodies are defined collectively by their bounding surface(s), cross-sectional (two-dimensional)

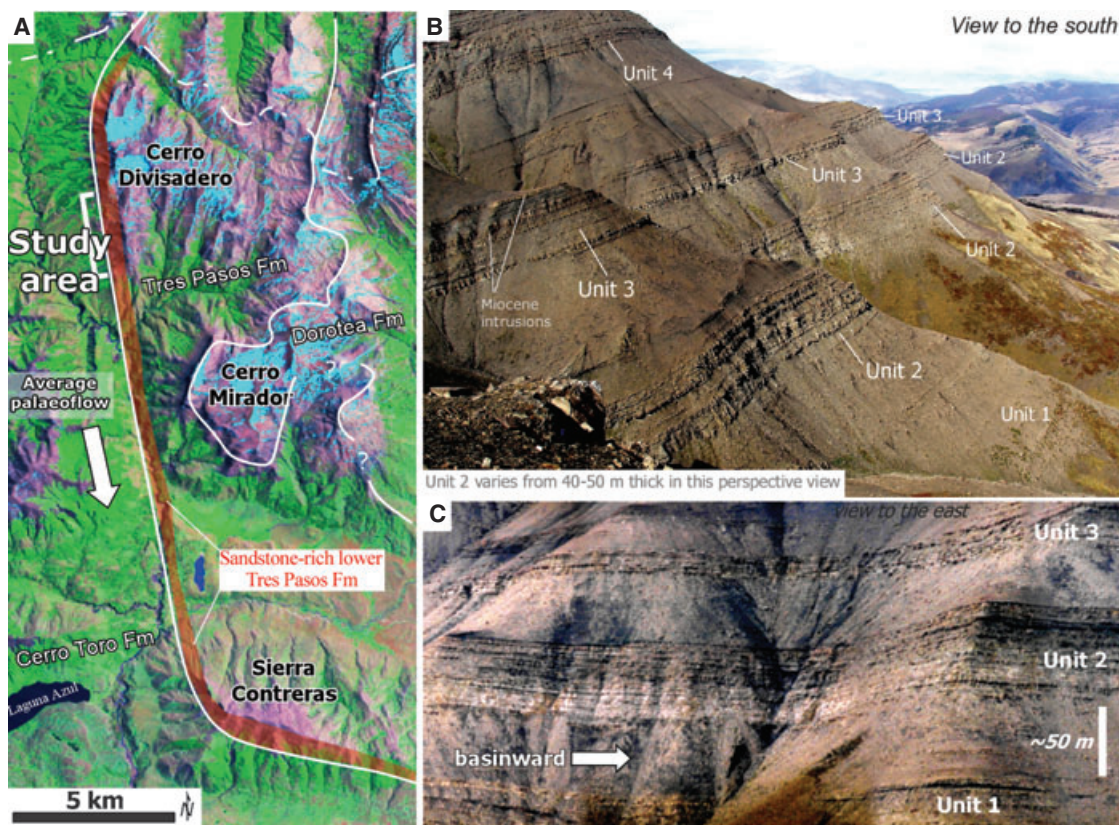


Fig. 4. (A) Satellite map of the Rio Zamora region in the Ultima Esperanza District of southern Chile. The international border is indicated by a dashed white line in the upper part of the map. The sandstone-rich lower part of the Tres Pasos Formation, shown in light red fill, crops out along the west face of a series of east-dipping ridges. The upper part of the formation (not studied in detail) is dominated by shale forming an extensive dip-slope exposure to the east up to base of Dorotea Formation. Palaeocurrents for the interval of interest are generally to the south to south-east. The focus area for this study is a 2.5 km long transect on the southern half of Cerro Divisadero. (B) Photograph looking to the south showing nature of the exposure. Over 600 m of deep-water stratigraphy is subdivided into four sandstone-rich units (informally Units 1 to 4) ranging in thickness from 20 to 70 m. Reddish-brown resistant layers are Miocene igneous sills. (C) Oblique aerial photograph of the upper parts of Unit 1 and Unit 2, and lower part of Unit 3. Lateral exposures in Units 2 and 3 are continuous for over 2 km. Photograph modified from Shultz *et al.* (2005).

geometry, internal facies and bedding architecture, sandstone richness, and degree of amalgamation. Of the four mappable sandstone packages present at Cerro Divisadero (Fig. 4B and C), Units 2 and 3 are the best exposed and least disrupted by post-depositional features and represent the focus of detailed analysis. Approximately 350 palaeocurrent measurements (derived primarily from sole marks) supplement the facies information and aid in reconstruction of the palaeogeomorphic setting.

Sandstone and geometry metrics

Measured sections, combined with sedimentary body correlations, provide a database from which to calculate quantitative metrics. This study

utilizes the abundant measured section data (>1800 m) to compute one-dimensional metrics of sandstone richness, degree of amalgamation and bed thickness. Additionally, high-resolution correlation of bedsets within the context of sedimentary bodies permits a quantitative evaluation of lenticularity.

Sandstone richness

Sandstone richness (commonly referred to as net sand or net-to-gross in the petroleum industry) has long been used to describe one-dimensional sections (outcrop or subsurface) of deep-water deposits. This measure can be expressed as a percentage or ratio. For this study, sandstone richness is defined as the thickness of sandstone divided by the total thickness of interval of

Table 1. Description of facies and facies associations, Tres Pasos Formation, Cerro Divisadero.

Facies association	Facies	Dominant grain-size	Sedimentary structures	Turbidite divisions*	Bounding surfaces	Thickness	Secondary features	Depositional process(es)
F1: Sandstone with minor siltstone	F1a	Very fine to lower medium-grained sandstone; siltstone commonly interbedded	Normally graded; structureless or plane-laminated to wavy/ripple-laminated	Partial to complete Bouma sequences	Sharp base; gradational to sharp top	Up to several metres (sed. units 5–30 cm)	Mudstone intraclasts rare; organic-rich detritus common in thin (<3 cm) layers on some bed tops	Mix of traction and suspension sedimentation from predominantly low-density turbidity currents
	F1b	Upper fine to upper-medium-grained sandstone	Normally graded; structureless; amalgamation of beds common	S ₃ /T _a	Sharp to erosive base; sharp top	Up to 20 m (sed. units 30–150 cm)	Mudstone intraclasts common at sed. unit bases; dewatering structures rare; loading and soft-sediment deformation rare	Rapid suspension sedimentation from high-density turbidity currents
	F1c	Upper medium to very coarse-grained sandstone and granules	Ungraded or normally graded; crude alignment of clasts	S ₁ , S ₃ , or none	Sharp to erosive base; gradational to sharp top	Up to 18 m (sed. units up to 70 cm)	Mudstone intraclasts abundant (up to 10 cm in length); centimetre-scale shell fragments abundant	Traction deposition from net-bypassing flows
F2: Shale with minor siltstone		Shale with minor siltstone	Structureless or faintly laminated	–	Gradational to sharp base; sharp top	Up to tens of metres	Thin (<5 cm) very fine to fine-grained sandstone beds rare	Hemipelagic settling and very dilute low-density turbidity currents
F3: Chaotic mudstone-rich deposits		Dominantly shale/siltstone; sandstone rare	None; discordant to chaotic; some soft-sediment deformation	–	Sharp discordant base; variable top	Up to 10 m	Commonly includes rafted blocks of siltstone or sandstone; disorganized pods of poorly-sorted sandstone	Mass wasting (sliding/slumping) and cohesive matrix-supported debris flow

*‘S’ divisions from Lowe (1982); ‘T’ divisions from Bouma (1962).

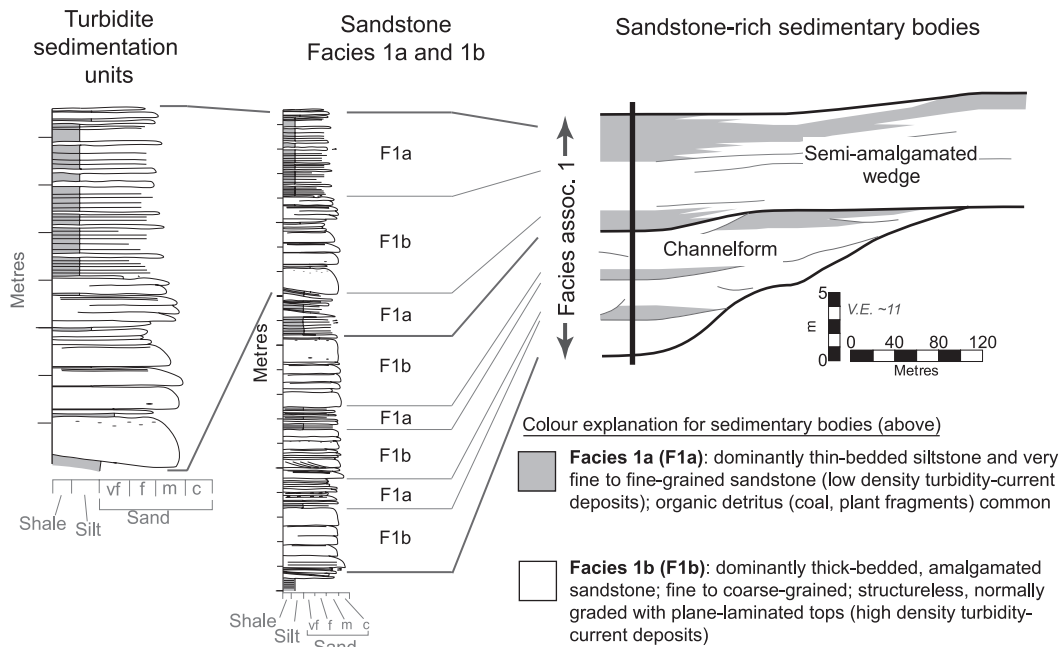


Fig. 5. A hierarchical approach combines sedimentological information from facies and facies associations within the context of sedimentary bodies, which are defined by distinct geometries and associated surface. Refer to Table 1 for detailed description of facies and facies associations.

interest and expressed as a fractional quantity between 0 and 1.

Amalgamation ratio

Amalgamation ratio (AR) is defined as the number of amalgamation surfaces (i.e. sandstone-on-sandstone contacts) divided by the total number of sedimentation units for a given interval. The AR concept utilized is essentially equivalent to that of Manzocchi *et al.* (2007) which is slightly modified after Chapin *et al.* (1994). For comparative ease, this is also expressed as a quantity between 0 and 1. The value of AR is that intervals with comparable sandstone richness may have significantly different degrees of amalgamation because of thin siltstone or shale partings separating sedimentation units.

Lenticularity index

Quantifying the geometry of lenticular sandstone bodies is an additional metric that can be used to compare and contrast sedimentary bodies within a deep-water succession. The method applied here, termed 'lenticularity index', is similar to the thickness change factor (TCF) described by Pickering & Hilton (1998) and Drinkwater & Pickering (2001). Lenticularity index is presented as a proportional quantity to facilitate comparison

among body types and with sandstone metrics. The thickness of each sedimentary body was determined at stations 200 m apart using correlation diagrams. The thickness change from each station was divided by the average thickness, resulting in a proportional thickness as a function of lateral position. Finally, an average of all proportional thickness measurements was determined for the entire sedimentary body. It is important to note that measurements derived from two-dimensional exposures of three-dimensional sedimentary bodies may limit the wide applicability of this metric and comparison to other systems.

SEDIMENTARY FACIES

The Tres Pasos Formation at Cerro Divisadero is subdivided into three facies associations, each several to tens of metres thick and defined by their dominant lithology: (i) sandstone with minor siltstone; (ii) shale with minor siltstone; and (iii) chaotic mudstone-rich deposits. The sandstone facies association is the main focus of this study and is subdivided into three component facies based primarily on grain-size, sedimentary structures and sedimentation unit thickness (Table 1 and Fig. 5).

Facies association 1 (F1): Sandstone with minor siltstone

Facies 1a: Thin-bedded sandstone and siltstone

Facies 1a (F1a) consists of fine-grained, thin-bedded (<0.3 m) sandstone, siltstone and shale (Table 1; Fig. 6). Sharp-based beds of structureless sandstone (Fig. 6A and B) contain the coarsest grain-size observed (lower medium). Occurrences of plane-laminated very fine-grained to fine-grained sandstone typically are interlaminated with siltstone or shale at the millimetre scale (Fig. 6C and D). Ripple-laminated to wavy-laminated very fine-grained to fine-grained sandstone is also present but is not as common (Fig. 6C). High concentrations of organic detritus,

in the form of fragments of coal or carbonaceous shale and woody material, are observed in F1a in very thin (<3 cm) layers (Fig. 6E and F). Plane-laminated to wavy-laminated siltstone is, in some cases, interbedded with the thin-bedded and finer-grained sandstone described above. More commonly, however, this siltstone facies is present as a distinct interval tens to hundreds of centimetres thick (Fig. 6A, B and D).

The majority of the deposits in F1a record mixed suspension and traction sedimentation associated with waning low-density turbidity currents. The thicker (10 to 20 cm) structureless beds represent suspension sedimentation from the high concentration bases of overall low-density turbidity currents (T_a division of Bouma,

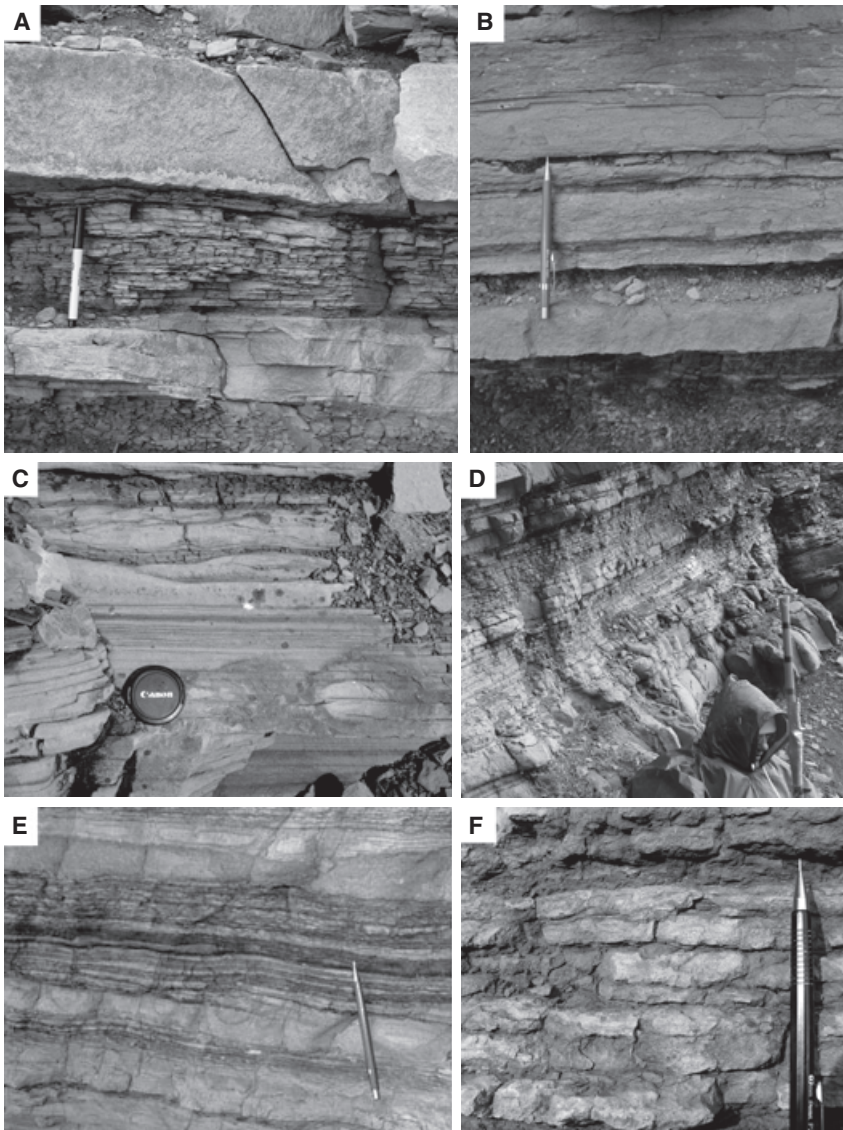


Fig. 6. Photographs of thin-bedded sandstone and siltstone facies 1a (F1a). (A) Fine-grained to medium-grained thin-bedded structureless sandstone, laminated siltstone to very fine-grained sandstone, and fine-grained plane-laminated sandstone. (B) Common assemblage of facies observed in F1a. (C) Wavy to ripple-laminated very fine-grained to fine-grained sandstone commonly associated with plane-laminated sandstone. Camera lens cap is 8 cm wide. (D) A ~2 m thick succession of F1a showing the interbedded character of this association. Note person for scale (divisions on Jacob staff are 10 cm). (E) Dark organic detritus (woody or plant material) is commonly concentrated in laminae and interbedded with siltstone. (F) Crudely laminated organic detritus-rich sandstone. Pens/pencils shown in (A), (B), (E) and (F) are 15 cm long.

1962). The plane-laminated and ripple-laminated sandstone is described by the T_b and T_c divisions of Bouma (1962), respectively (Table 1). The laminated siltstone-dominated successions are the product of dilute low-density turbidity currents (T_d divisions of Bouma, 1962).

Facies 1b: Thick-bedded, amalgamated sandstone

Facies 1b (F1b) consists largely of thick-bedded (≥ 0.3 to 2.0 m) medium-grained to coarse-grained sandstone (Table 1; Fig. 7). Sandstone beds are typically structureless and normally graded; mudstone intraclasts are common in the basal parts of some beds (Fig. 7A and B). In some cases, plane-laminated, fine-grained sandstone is preserved at the top of sedimentation units. Laterally, sedimentation unit thickness, sandstone richness and degree of amalgamation can vary significantly. Vertical alternation of F1a and F1b is observed commonly in the upper parts of thick (>5 m) sandstone-rich intervals (Fig. 7C and D).

Facies 1b deposition records the highest flow energy and/or degree of confinement recognized in the Tres Pasos Formation at Cerro Divisadero. F1b is dominated by deposits of high-density turbidity currents (*sensu* Lowe, 1982). Lack of internal sedimentary structures and normal grading indicate rapid sedimentation from suspension (S_3 division of Lowe, 1982; T_a division of Bouma, 1962). Crude sedimentary structures (faint plane to low-angle cross-lamination) in the bottom or middle part of sedimentation units indicate traction sedimentation (S_1 division of Lowe, 1982) but are only rarely preserved. Fine-grained to medium-grained plane-laminated sandstone in upper parts of sedimentation units indicates traction sedimentation related to a waning low-density turbidity current phase of deposition (i.e. T_b division of Bouma, 1962).

Facies 1c: Mudstone intraclast and shell fragment-rich sandstone

Facies 1c (F1c) consists of coarse-grained to very coarse-grained sandstone with granules and abundant centimetre-scale shell fragments and/or mudstone intraclasts (up to 10 cm in length; Fig. 8). The concentration of shell fragments decreases upward within an individual bed in most cases. Internal stratification (crude alignment of intraclasts and/or shell fragments) is observed in some cases. Sedimentation units are typically 30 to 50 cm thick but multiple

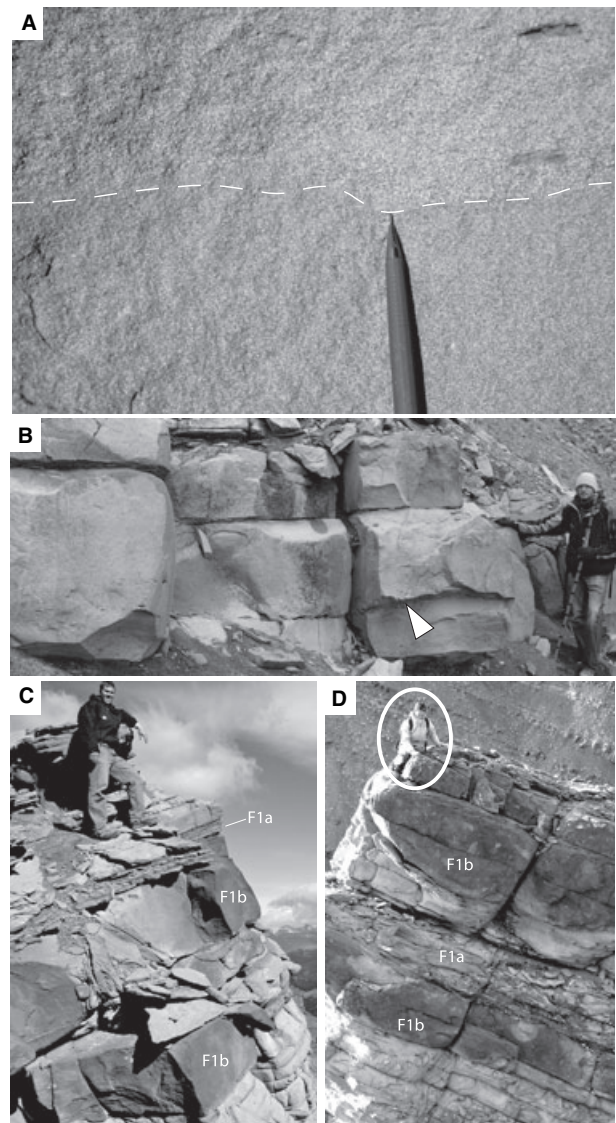


Fig. 7. Photographs of thick-bedded, amalgamated sandstone facies (F1b). (A) Dashed white line denotes amalgamation surface between underlying fine-grained structureless sandstone sedimentation unit and overlying medium-grained sandstone sedimentation unit containing sparse mudstone intraclasts near base. Pencil is 15 cm long. (B) Representative bedding style and bed thickness of F1b. White arrow denotes amalgamation surface marked by mudstone intraclasts that have eroded out. Person is 1.8 m tall. (C) and (D) F1b is commonly interbedded with finer-grained, thinner-bedded F1a at the bedset scale. Person in (C) is 1.9 m tall. Person circled in (D) is 1.7 m tall.

sedimentation units stack to form an interval up to 10 to 20 m thick that can be traced several hundred metres across the outcrop (Fig. 8A). These deposits are interpreted as the S_1 and S_3 divisions of high-density turbidity currents (Lowe, 1982).

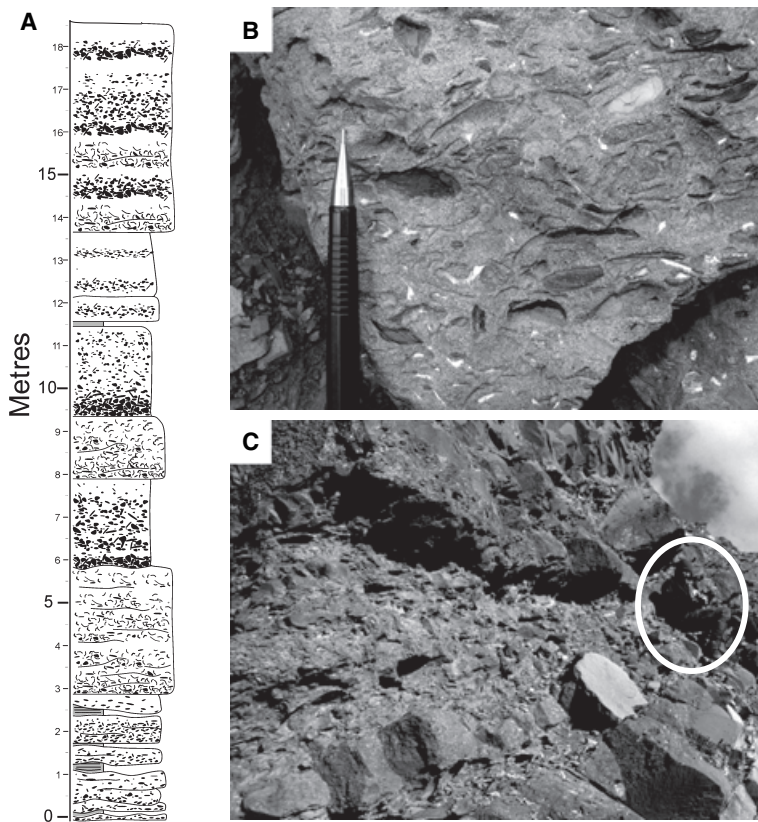


Fig. 8. Photographs of shell fragment-rich, coarse to very coarse-grained sandstone facies (F1c). (A) Measured section showing 18 m thick succession of beds dominated by F1c. (B) Close-up photograph showing abundant shell fragments. Pencil is 15 cm long. (C) Bed-scale view of F1c shows bedded nature. Successions of F1c range in thickness from < 2 m to nearly 18 m. Person at right (sitting) circled is 1.9 m tall.

Facies association 2 (F2): Shale with minor siltstone

This facies association consists almost entirely of massive to laminated concordant shale and is the dominant constituent of thick (30 to 80 m) intervals present between the four sandstone-rich units that collectively make up over half of the total thickness of Tres Pasos Formation strata at Cerro Divisadero (Fig. 4B and C; Table 1). Siltstone and thin (< 5 cm) beds of very fine-grained sandstone are rare and typically occur in close stratigraphic proximity (within 5 to 10 m) to the major sandstone-rich successions. This facies association is dominated by deposits from hemipelagic sedimentation or very dilute, low-density sediment gravity flows. The boundary between F2 and underlying strata is typically gradational over a few to several metres of thickness, whereas the upper boundary is commonly, but not always, sharply overlain by F1 or, in some cases, mudstone-rich mass transport deposits of facies association 3.

Facies association 3 (F3): Mass transport and debris flow deposits

Facies association 3 (F3) generally is mudstone-rich with sparse and disorganized sections of

siltstone and/or sandstone (Fig. 9). Discordant shale or siltstone and poorly sorted mudstone/siltstone make up the bulk of F3 (Table 1). Discordant blocks of shale and siltstone that typically show evidence of soft-sediment deformation also are common (Fig. 9A, C and D). Discrete blocks of strata range in scale from less than a metre to several metres in diameter. Contacts between discordant sections show no evidence of erosional truncation and commonly are disorganized to unrecognizable (Fig. 9C and D). Internally, these discordant blocks display a range of soft-sediment deformation from nearly intact and displaced (Fig. 9C and D) to chaotically folded and deformed blocks (Fig. 9A). These characteristics suggest complex sliding and/or slumping processes that are not associated with complete disaggregation of material during transport. The primary sedimentological characteristics of the transported blocks are similar to those described for F1a (Fig. 9D).

Poorly sorted mixtures of shale, silt and fine sandstone in various proportions are also common to F3. The most characteristic occurrence consists of a poorly sorted silt matrix with small (< 1 m) diffuse and disorganized 'pods' of fine sandstone-rich material (Fig. 9B). There is no organization or sedimentary structures apparent

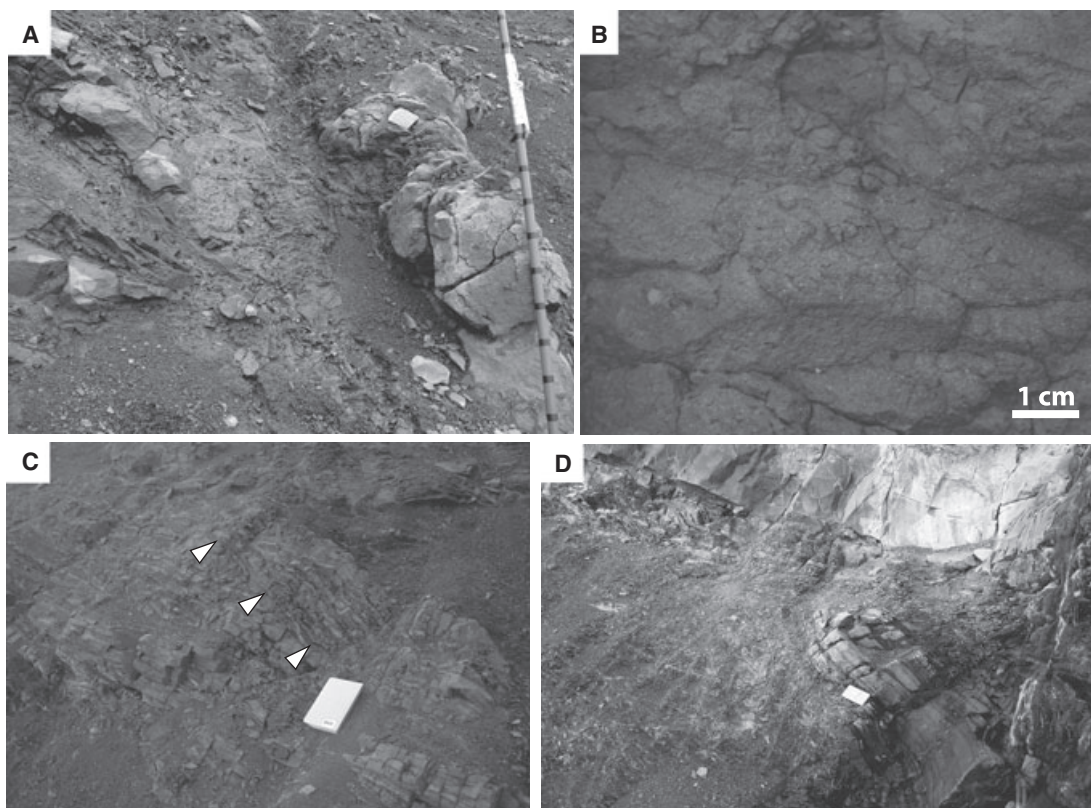


Fig. 9. Photographs of fine-grained facies associated with chaotic facies association 3 (F3). (A) Injected sand is commonly associated with chaotic, discordant shale/siltstone. Increments on Jacob staff are 10 cm. (B) Siltstone to fine-grained sandstone-rich debris flow deposit. (C) Discordant shale and siltstone. White arrows point to angular surface separating blocks. (D) Rafted blocks of siltstone are, in some cases, present directly underlying thick packages of F1b. Field notebook in (C) and (D) is 18 cm long.

internally and boundaries typically are gradual with the discordant blocks. These deposits are interpreted as the product of debris flow processes (Middleton & Hampton, 1973, 1976; Lowe, 1982). Vertical or near-vertical columns of injected sandstone up to 1 to 2 m thick (Fig. 9A; Table 1) are rare within F3 but provide further evidence for soft-sediment remobilization. Because of the mudstone-rich nature of these strata, sedimentary bodies are not exposed as well as sandstone-rich units, thus making it difficult to document their scale, extent and geometry.

SEDIMENTARY BODIES

Sedimentary bodies, or depositional elements, are the fundamental building blocks that make up a deep-water succession (Mutti & Normark, 1987, 1991; Pickering *et al.*, 1995). Characterizing the geometry, spatial configuration (i.e. architecture) and palaeoflow attributes of sediment gravity flow deposits within the context of sedimentary bodies is essential for interpreting the palaeogeomorphic

evolution of a system. The sandstone-rich intervals at Cerro Divisadero crop out as discrete, shale-encased bodies ranging from a few metres to greater than 20 m thick, with distinct bounding surfaces. Characterizing bounding surfaces and geometry have long been recognized as key aspects of sedimentary body analysis in general (e.g. Miall, 1985) and in deep-water strata specifically (e.g. Pickering *et al.*, 1995; Clark & Pickering, 1996; Gardner *et al.*, 2003; Anderson *et al.*, 2006; de Ruig & Hubbard, 2006). Although these fundamental bodies generally are comparable with architectural or depositional elements documented in other outcrop or subsurface studies, they are used here to characterize the evolution of this system and may not be directly analogous to other deep-marine slope systems. Moreover, preserved sedimentary bodies record a combination of processes and geomorphic conditions over time and thus rarely represent a single geomorphic element.

Five sedimentary body types are recognized at Cerro Divisadero: (i) channelform-fill; (ii) amalgamated sheet; (iii) semi-amalgamated wedge;

(iv) non-amalgamated wedge; and (v) mass transport deposit. With the exception of mass transport deposits, these body types are defined by cross-sectional (two-dimensional) geometry, internal facies distribution, internal bedding architecture, sandstone richness and amalgamation ratio. These attributes are evaluated qualitatively for the entire succession and quantitatively for Units 2 and 3 (Fig. 10). General categories of sandstone richness, termed high, medium, and low, have ranges of >0.8 , 0.5 to 0.8 and <0.5 , respectively.

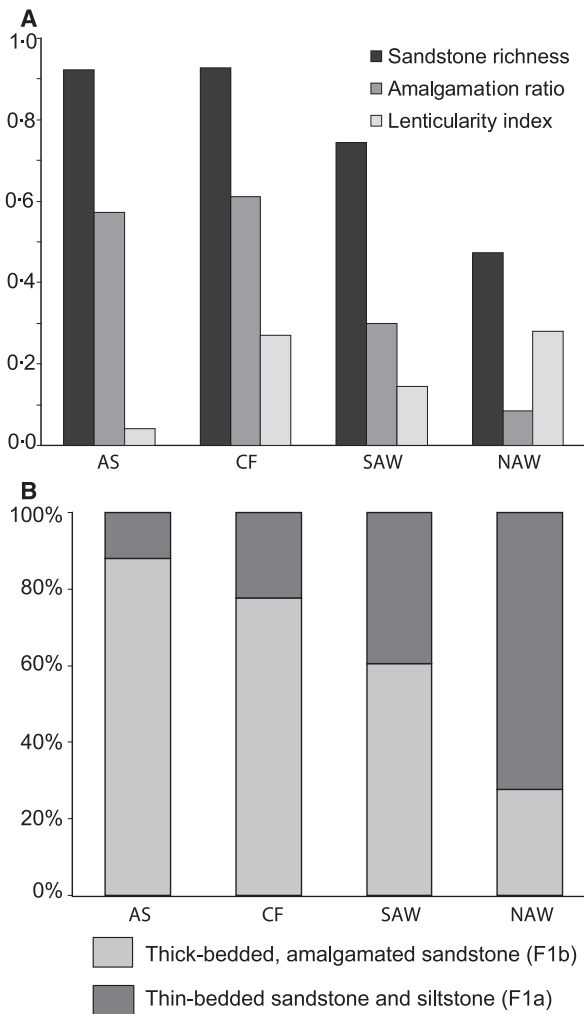


Fig. 10. Graphs summarizing average values of quantitative metrics for four sedimentary body types documented in Units 2 and 3 (AS, amalgamated sheet; CF, channelform-fill; SAW, semi-amalgamated wedge; and NAW, non-amalgamated wedge). (A) Average values of sandstone richness, amalgamation ratio, and lenticularity index for each sedimentary body type. Indices are shown between 0 and 1 for comparison. Refer to text for explanation of metric determination. (B) Graph showing relative proportion of sandstone facies (F1a and F1b) for each sedimentary body type. See Table 2 for summary of metrics organized by stratigraphic unit.

Amalgamation ratio is similarly subdivided into high (>0.5), medium (0.2 to 0.5) and low (<0.2) (Fig. 10).

Channelform-fill

Characterization of channel-filling successions in deep-water outcrops is an active area of deep-water research (Campion *et al.*, 2000; Hickson & Lowe, 2002; McCaffrey *et al.*, 2002; Gardner *et al.*, 2003; Beaubouef, 2004; Hubbard *et al.*, 2008). For this study, the channelform-fill (CF) sedimentary body type is based on a lenticular geometry (lenticularity index >0.2), internal facies distribution and internal bedding architecture (Fig. 10). The genetic inference of channelization for this body type is derived primarily from evidence for significant erosional truncation of underlying strata. The underlying strata are typically shale-rich deposits genetically unrelated to the development of the overlying channelform body and its fill. The basal erosional surface is not a single bypass surface but a composite surface that, in some locations, is expressed as a cluster of multiple surfaces. This observation suggests that the feature was a conduit for numerous sediment gravity flows over a period of time and not the product of a single event (e.g. large scour). Deposits in the basal part of CFs onlap and/or pinch out against the basal erosional surface. The nature of the fill is highly variable and can be quite complex, as evidenced by abundant smaller-scale cut-and-fill features and juxtaposition of F1a and F1b.

Amalgamated sheet

The definition of this sedimentary body type is based largely on the occurrence of a thick (>20 m) tabular, sheet-like body (at the scale of the 2.5 km long outcrop) that is very sandstone-rich (>0.9) and has a high degree of amalgamation (amalgamation ratio >0.8 ; Fig. 10). A lateral change from more to less amalgamated sandstone (i.e. from F1b to F1a) is an important characteristic of this body type. Internal scouring and channellization similar in scale to that observed internal to the channelform body are recognized only rarely.

Semi-amalgamated and non-amalgamated wedges

The semi-amalgamated wedge (SAW) body type is based primarily on cross-sectional geometry (lenticularity index >0.1) and degree of amalgamation

(amalgamation ratio 0.2 to 0.5; Fig. 10). The wedge shape is typically achieved over the lateral scale of tens to hundreds of metres and is a result of one or a combination of the following: (i) depositional thinning and/or complete pinching out of sandstone beds or bedsets of F1a into more siltstone-rich deposits; (ii) onlap and filling of small, shallow (<5 m) topographic depressions; or (iii) truncation of upper boundary of body by overlying erosional surface. Internally, beds or bedsets commonly exhibit laterally offset (i.e. compensational) stacking. Less common are internal channel-fill or scour-fill elements.

Non-amalgamated wedges (NAWs) are similar to SAWs in terms of geometry but are typically thinner (3 to 6 m) and less amalgamated (amalgamation ratio <0.1; Fig. 10). Non-amalgamated wedges have a low proportion of thick bedded, amalgamated sandstone (F1b) and, in some cases, are dominantly siltstone with some very fine-grained sandstone beds. Internally, NAWs exhibit similar patterns to semi-amalgamated wedges although typically at a smaller scale.

Mass transport deposit

Mass transport deposits (MTDs) are readily distinguishable from the other sedimentary bodies because of their mudstone-rich and internally disorganized nature. This body type has a direct relationship with the facies association (F3) that describes it. MTD bodies do not exhibit a repeated or systematic shape and appear to grade into concordant shale (F2) in some cases. The most extensive MTDs at Cerro Divisadero (>10 m in lateral extent) occur in shale-rich intervals that are not exposed well enough to precisely map the full extent and geometry.

STRATIGRAPHIC EVOLUTION

Patterns of facies distribution and types of sedimentary bodies are evaluated for each of the four stratigraphic units. The stratigraphic 'sub-units' within each unit (e.g. 2a, 2b, 3a, 3b) represent one of the five sedimentary body types. Interpretations of depositional processes and setting are summarized through an analysis of the lateral and vertical relationships within and among the sub-units.

Unit 1

Unit 1 is the lowest sandstone-rich succession exposed at Cerro Divisadero (Fig. 4C). The strata

underlying this unit (lithostratigraphically, the uppermost part of the Cerro Toro Formation) are dominated by shale and mudstone-rich MTDs. Unit 1 outcrops are limited in extent, typically exposed well only in gullies, and otherwise covered by vegetation or talus, making documentation of lateral relationships difficult. Despite this limitation, sedimentological and bed-scale observations at multiple sites reveal important characteristics. Thick-bedded sandstone (F1b) is present but rarely in stacked amalgamated intervals (>5 m thick) that typically characterize this facies. Erosional features are rare and of low relief (<2 m) and sedimentological evidence for significant bypass (e.g. lag deposits) is rare. Bed-scale compensation of the wedge-shaped sedimentary bodies is observed at multiple locations. Evidence for MTDs is common to abundant in the fine-grained intervals between sandstone-rich bodies. Mudstone-rich debris flow deposits are particularly abundant in the MTDs of Unit 1 relative to overlying units.

The presence of multiple intervals of mudstone-rich MTDs indicates that this was a site of deposition for numerous mass wasting events. The characteristics of the sandstone bodies indicate that this area was not a major and/or long-lived conduit for coarse-grained flows. The bed-scale compensation within these metre-scale bodies suggests flows that are weakly confined to unconfined that construct lobate bodies (cf. Mutti & Ghibaudo, 1972). These deposits could be interpreted as representing either an area lateral to a conduit, in an out-of-channel position, or relatively distal within a channel-lobe system. Topography created by the abundant MTDs probably exerted a primary control on the distribution of sandstone bodies in Unit 1.

Unit 2

Unit 2 (42 to 55 m thick) is well-exposed across the entire study area and is subdivided into two main sub-units, 2a and 2b (Fig. 11). The lower sub-unit 2a is described as an amalgamated sheet based primarily on high sandstone richness (i.e. high proportion of F1b) and overall tabular geometry at the scale of investigation (Fig. 11). The strata underlying sub-unit 2a in the north (measured sections 'A' and 'B') consist of discontinuous, small-scale (tens of metres) lenticular sandstone bodies that represent filling of low-relief scours or channels. The presence of coarse-grained lag deposits throughout these bodies suggests a mixture of bypass and deposition. The

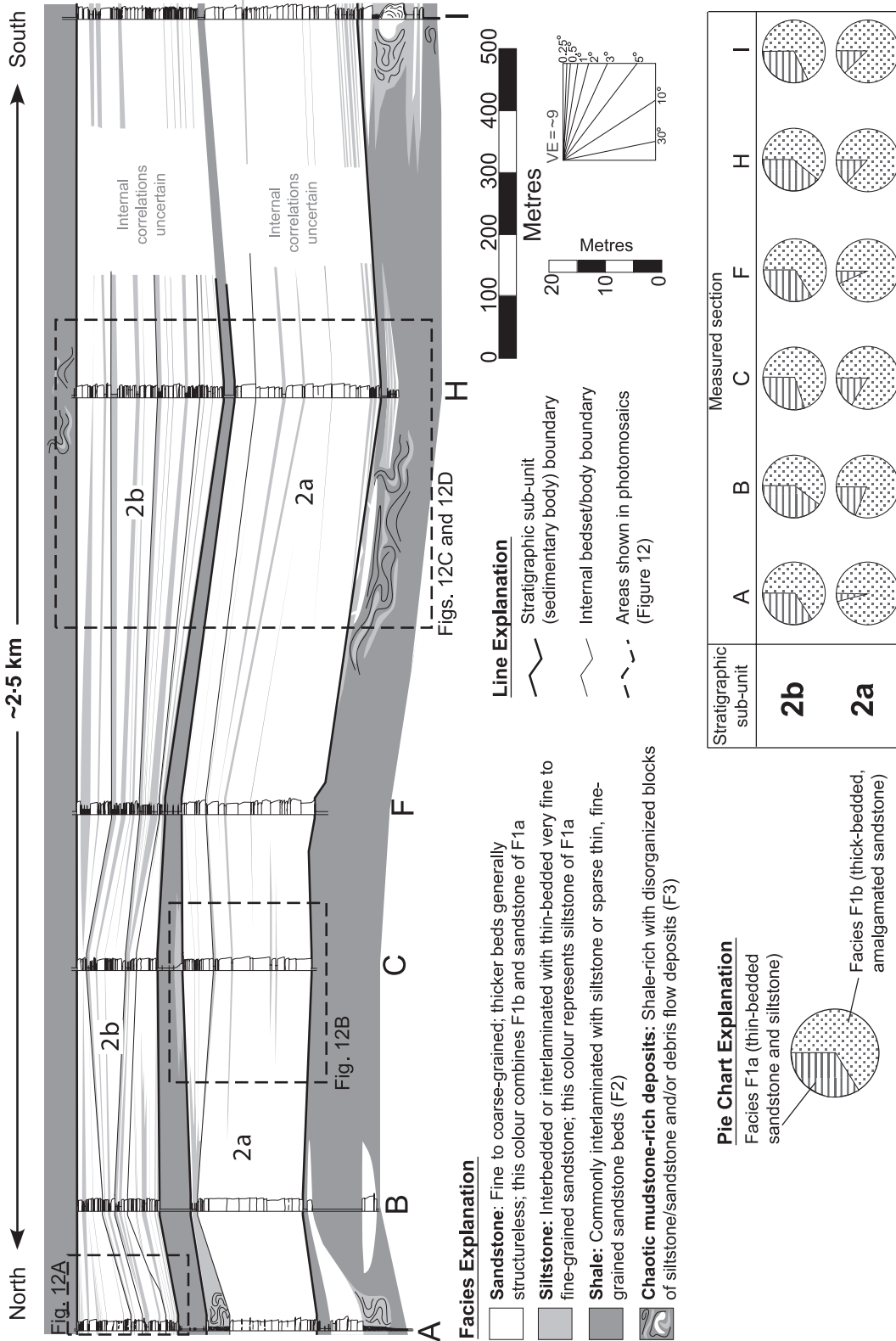


Fig. 11. Correlation diagram of sandstone-rich Unit 2 showing six measured sections (A to I) across > 2 km outcrop transect. Measured sections were correlated physically in the field and/or through photomosaic mapping. Regional palaeo-slope is to the south (right). Colour scheme shows all sandstone as white to emphasize sand architecture. Distribution of F1a and F1b is shown in pie charts for each measured section for the two stratigraphic sub-units (2a and 2b). Unit 2a is described as an amalgamated sheet (AS) based on its overall tabular geometry, high sandstone richness and high degree of amalgamation. Thick-bedded, amalgamated sandstone (F1b) makes up at least 80% of all measured sections within this body. Unit 2b is described as a semi-amalgamated wedge (SAW) based on the overall southward increase in thickness and internal variability in bedding geometry and sandstone facies distribution. Refer to Fig. 12 for photographs of areas denoted by dashed boxes and Table 2 for summary of sandstone richness, amalgamation ratio, and lenticularity index values for Unit 2.

occurrence of MTDs underlying sub-unit 2a increases markedly to the south (Figs 11 and 12C). The bottom half of sub-unit 2a exhibits lateral facies changes from completely amalgamated sandstone (F1b) to non-amalgamated sandstone (F1a) over distances of tens to hundreds of metres (Fig. 12B). In some cases, amalgamation

surfaces can be tracked across the exposure with no evidence of truncation or scouring (Fig. 12B). Palaeocurrent indicators at the base of sub-unit 2a are all directed within the south-east quadrant (Fig. 11) but show significant variation locally. For example, palaeocurrent directions from the north side of the cliff face shown in Fig. 12B are

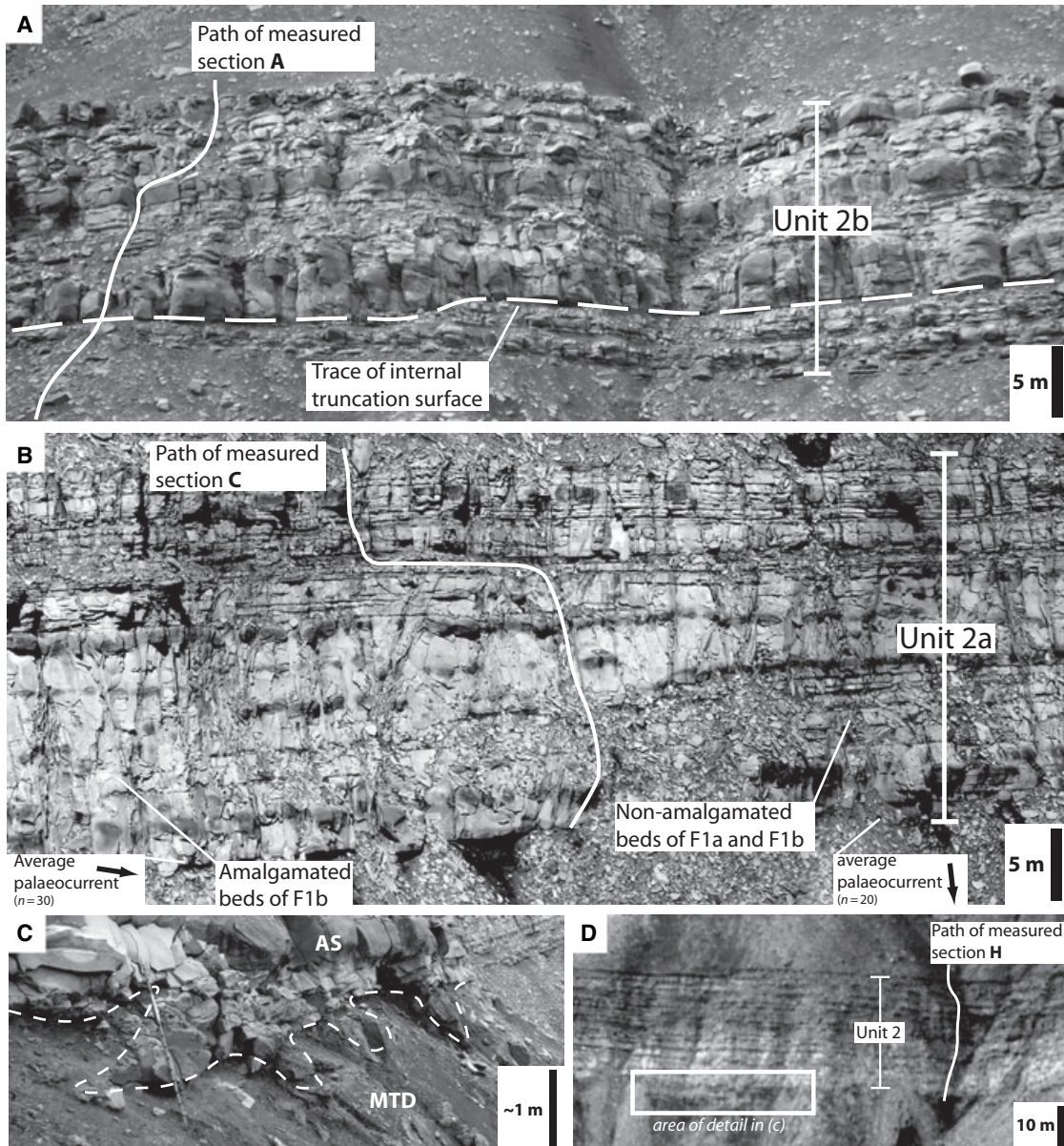


Fig. 12. Photomosaics of cliff-face exposures of Unit 2 showing internal architecture and relationships of F1a and F1b to sedimentary bodies. See correlation diagram in Fig. 11 for location and measured sections. (A) Unit 2b at northernmost measured section. Note surface that truncates underlying beds of F1a (dashed white line) within body. Small-scale bodies stack to form Unit 2b which is defined as a semi-amalgamated wedge (SAW). (B) Unit 2a at measured section C. Note lateral change in lower half of body from completely amalgamated beds of F1b at the left to a mix of non-amalgamated beds of F1b and F1a to the right of the measured section path. Amalgamation surfaces can be traced through this thick sandstone package which is defined as an amalgamated sheet (AS). Palaeocurrent indicators on basal sandstone beds vary by as much 90° over a distance of tens of metres. Close-up (C) and aerial view (D) of mudstone-rich MTDs underlying Unit 2 at measured section H. Note complex basal boundary juxtaposing F1b against MTDs. Note Jacob staff at left in (C).

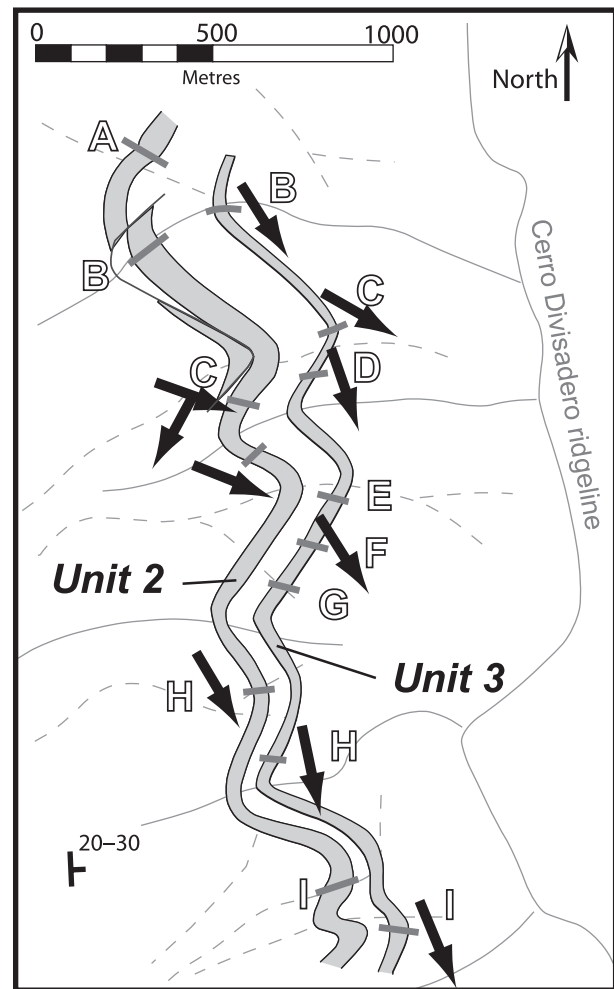
nearly due east, whereas measurements ~ 100 to 150 m to the south are south to south-east, diverging nearly 90° .

Amalgamated sheet deposits of sub-unit 2a are interpreted as a proximal lobe complex within a channel-lobe transition zone. The high degree of amalgamation is consistent with conditions where sand-laden flows consistently deposit the high-density part of the flow. Branching and bifurcating of smaller erosional features are typical in channel-lobe transition zones observed in modern systems (Mutti & Normark, 1987; Wynn *et al.*, 2002). The internal variability of amalgamation and evidence for small-scale (1 to 3 m) scour and fill features documented in sub-unit 2a are consistent with these observations. Additionally, the diverging palaeocurrent patterns corroborate the interpretation of branching flow paths that might reflect a distributive system. The southward change from more to less internal channellization represents a gradational boundary within the channel-lobe transition zone. The increased occurrence of MTDs to the south (down-dip) (e.g. Galloway, 1998) in conjunction with evidence for diminished channellization (e.g. Mutti & Normark, 1987) suggests that the southern area had a relatively lower gradient during sand deposition.

The overlying sub-unit 2b is described as a semi-amalgamated wedge body type. It is separated from the underlying sub-unit by a 2 to 6 m thick shale and siltstone interval that is continuous across the entire study area (Fig. 11). Although the proportions of F1a and F1b remain constant from north to south (Fig. 11), the characteristics of the internal architecture indicate more channellization in the north (Fig. 12A). Evidence of laterally offset stacking of smaller-scale wedge-shaped bedsets is observed between measured sections B, C, and F (Fig. 11). Further south, near measured section H, the internal bedding architecture is more tabular (Fig. 12D).

Sub-unit 2b records continued deposition and infilling of the original site of accommodation (sub-unit 2a) following a period of cessation of sand deposition (marked by a siltstone interval that separates the sub-units). This period of siltstone deposition might signify an avulsion of the sand delivery system away from this site. The higher proportion of F1a in sub-unit 2b indicates that flows are focused nearby (either up-dip and/or laterally), but not directly at this site as in sub-unit 2a. The upper boundary of Unit 2 varies from site to site, but most commonly is characterized by a sharp boundary with overlying concordant shale (F2) and, in a few locations, MTDs (F3;

Fig. 11). This sharp, non-erosional upper contact suggests an avulsion process similar to the upper boundary of sub-unit 2a. Palaeocurrent directions for Unit 2 average 125° which is the most easterly of the entire succession (Fig. 13A). The modest



Explanation




-  Trace of outcrop for Units 2 and 3
-  Measured section
-  Average palaeocurrent direction

Fig. 13. Map showing extent of outcrop and measured sections for sandstone-rich Units 2 and 3. Arrows represent average palaeocurrents from the base of the unit. Although outcrop is generally parallel to sediment transport direction, the ridge and gully topography provides smaller-scale three-dimensionality. Note diverging palaeocurrents at measured section C for Unit 2. See Figs 11 and 14 for correlation diagrams of Units 2 and 3, respectively.

thickening of both sub-units to the south probably represents a combination of downdip and lateral relationships in this proximal lobe complex. It is unclear from these data whether the east to south-east dispersal pattern reflects local sea-floor topography (e.g. MTDs) or a more system-wide influence (e.g. diversion of turbidity currents at the base of slope). The channel-lobe transition zone interpreted here is not similar in scale to channel-lobe transition zones associated with large, canyon-fed fans (e.g. Wynn *et al.*, 2002). This lobe complex is probably a smaller and shorter-lived feature scaled to the type of slope channel feeding it (e.g. Adeogba *et al.*, 2005; Johannessen & Steel, 2005).

Unit 3

Unit 3 contains the most lenticular and internally variable sandstone bodies documented at Cerro Divisadero. This study focuses on the lowermost of five sub-units (3a and 3b; Fig. 14). The lower sub-unit 3a has a maximum thickness of 26 m and is present only in the southern half of the study area as a result of pinching out of the body towards the north-east (Fig. 14). The basal bounding surface is a composite erosional surface that shows evidence for truncation of the underlying shale-rich strata. The presence of thin (<10 cm), discontinuous pockets of coarse-grained lag deposits along this surface suggests bypass and erosion. The entire body pinches out by progressive onlap of the basal deposits against this composite surface (Fig. 14). Beds directly above the basal bounding surface pinch out over short distances (<20 m), some of them directly onlapping underlying shale and some grading into mudstone intraclast-rich sandstone. Figure 15 shows distribution of facies and bedding architecture for sub-units 3a and 3b in the area where 3a completely pinches out. The internal architecture of sub-unit 3a is characterized by complex cut-and-fill features that juxtapose F1a and F1b (Fig. 15C). Although sub-unit 3a has the highest proportion of F1b within all of Unit 3, it is not as high as in underlying Unit 2 (Figs 11 and 14). Approximately 600 m to the south (at measured section H), a similar pattern of onlapping bedsets is observed (Fig. 16). This area also has the thickest occurrence of sub-unit 3a and has the highest proportion of F1b (Fig. 14).

Sub-unit 3a is described here as a channelform-fill sedimentary body that records the formation and subsequent filling of a submarine channel.

This interpretation is based primarily on the truncation of underlying strata and by the onlapping internal architecture. Palaeocurrent data for this sub-unit indicate a consistent south to south-east orientation averaging 170° (Fig. 13B). The correlation diagram in Fig. 14 is thus an oblique view, with the southward thickening of sub-unit 3a reflecting a more axial position of the channel-fill relative to sediment transport direction. The increase in the proportion of thick-bedded, amalgamated sandstone (F1b) from the margin (measured sections F and G; Fig. 15) towards the axis (measured section H; Fig. 16) is summarized by the pie charts in Fig. 14. The internal cut-and-fill architecture (e.g. Fig. 15C) reflects a history of erosion and bypass combined with deposition as the accommodation created by the initial channelization is filled. The scale of this channel-fill body is impossible to measure directly because it is larger than the outcrop. If measured section H is presumed to be the axis and the body is symmetrical, the entire complex is at least 1 km wide.

Sub-unit 3b, defined as a semi-amalgamated wedge, directly overlies and is distinguished from channelform-fill 3a by: (i) a widespread stratigraphic surface (traced between the sections in Figs 15 and 16); (ii) the overall geometry of the sedimentary body; and (iii) internal characteristics. Unlike Unit 2, which has a mappable siltstone interval between the sub-units, the bounding surface between 3a and 3b is more variable and, in some cases, characterized by direct sandstone-on-sandstone contact (Figs 14 to 16). Sub-unit 3b is present across the entire study area and is less lenticular than channelform-fill 3a. Internally, sub-unit 3b exhibits evidence for lateral changes of facies as a result of depositional thinning of individual sandstone beds (Fig. 15A), as well as compensational stacking of smaller-scale bodies (Fig. 16). Although the proportion of facies varies significantly across the study area, sub-unit 3b generally is richer in thin-bedded turbidites (F1a) (Fig. 14).

The lateral facies changes, laterally offset bodies and greater proportion of F1a in sub-unit 3b reflect flows that are less confined relative to channelform-fill 3a. Together, these two sedimentary bodies form a larger complex that reflects the filling of accommodation that initially formed as a result of channelization. As the channelform accommodation was filled (sub-unit 3a), subsequent flows responded to a diminished gradient and smoother topography as a result of preceding deposition (sub-unit 3b). Although impossible to unequivocally document at this outcrop, this

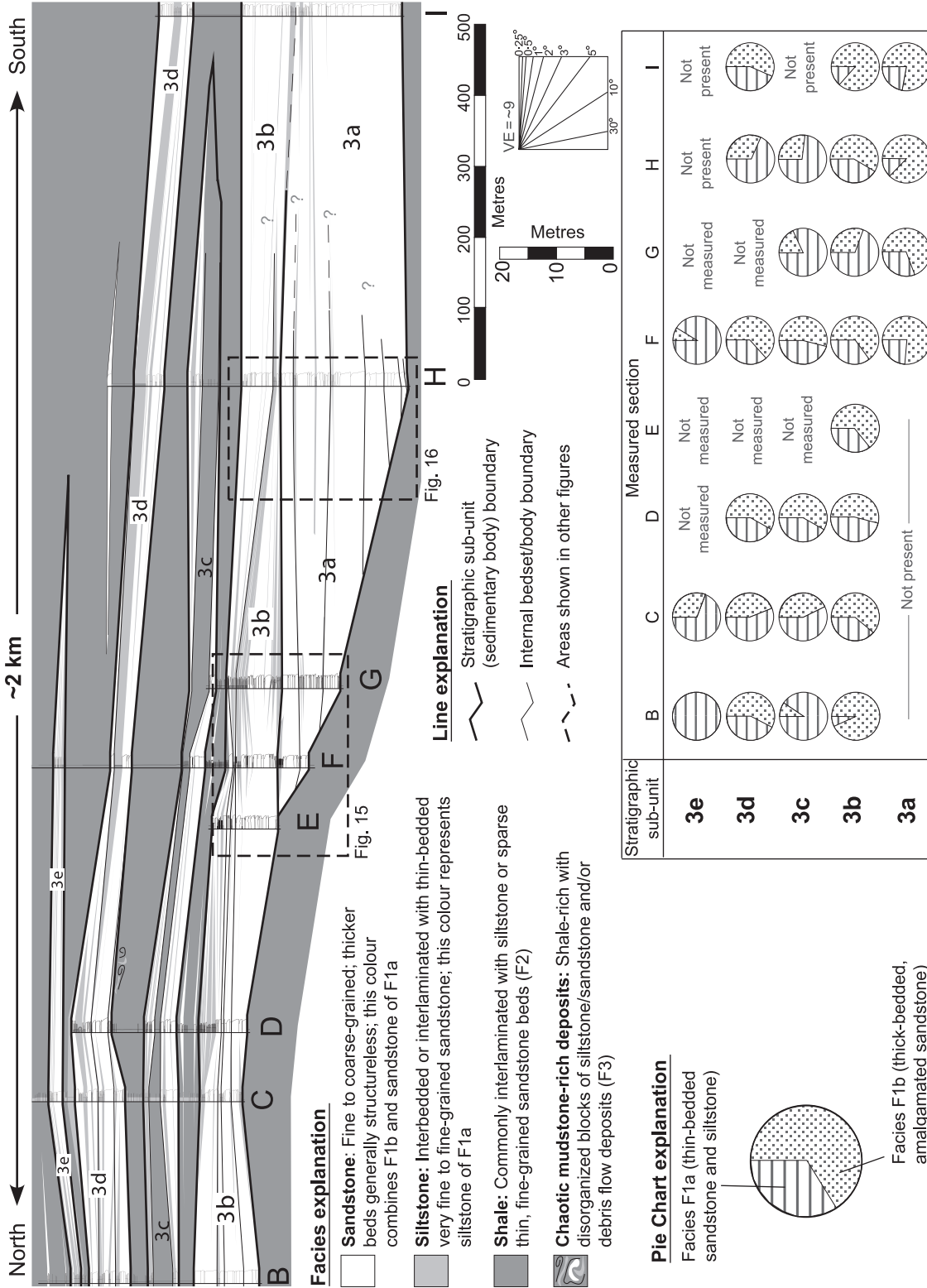


Fig. 14. Correlation diagram of Unit 3 showing eight measured sections (B to I) across > 2 km outcrop transect. Measured sections were correlated physically in the field and/or through photomosaic mapping. Regional palaeo-slope is to the south (right). Colour scheme shows all sandstone as white to emphasize sand architecture. Distribution of F1a and F1b is shown in pie charts for each measured section for the five stratigraphic sub-units (3a to 3e). Refer to Figs 15 and 16 for details regarding internal distribution of F1a and F1b and architectural style. See Table 2 for summary of sandstone richness, amalgamation ratio, and lenticularity index values for Unit 3.

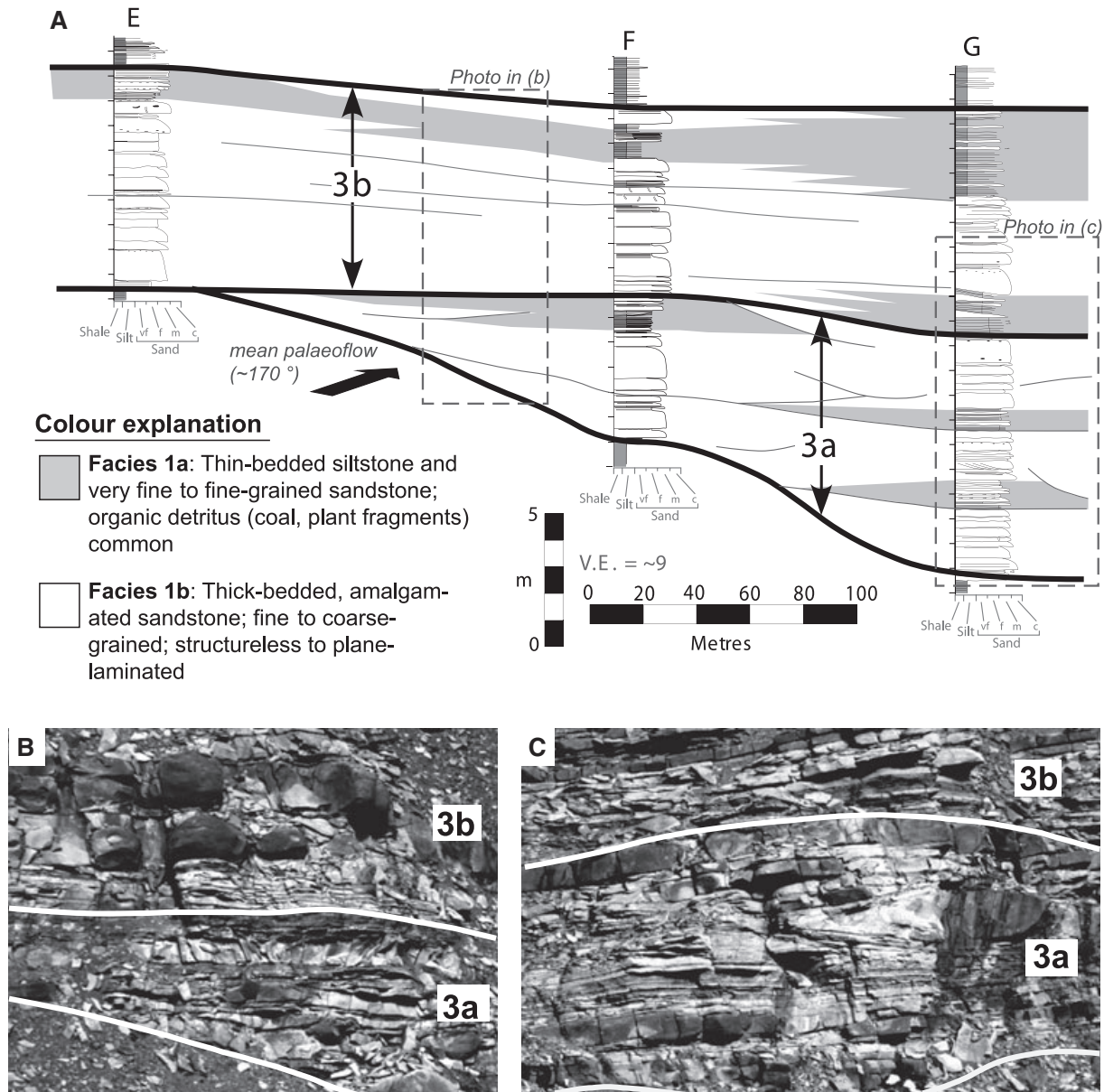


Fig. 15. (A) Correlation panel showing distribution of F1a and F1b for stratigraphic sub-units 3a and 3b in central part of study area (measured sections E, F and G). Average palaeocurrent direction is south to south-east (obliquely into face). Note pinch-out of sub-unit 3a, which is defined as a channelform-fill sedimentary body, to the north-east (left). Basal bounding surface is a composite surface showing evidence for truncation of underlying strata. Directly overlying this surface in some locations are thin (< 10 cm), discontinuous pockets of coarse-grained lag deposits. The internal bedding architecture of sub-unit 3a is characterized by small-scale (< 1 to 2 m) cut-and-fill features. The overlying sub-unit 3b is defined as a semi-amalgamated wedge and exhibits less lenticularity overall and internally. Lateral changes in sandstone facies evidenced by depositional thinning and/or pinching out of sandstone beds. (B) Photograph showing nature of pinch-out of channelform-fill 3a. (C) Photograph highlighting internal cut-and-fill architecture of channelform-fill 3a. Refer to Fig. 14 for correlation diagram of Unit 3 across study area. Figure simplified from Romans *et al.* (2007).

stacking pattern is probably a result of migration of the axial part of the system away from this site. In terms of depositional environment and sea-floor morphology, this semi-amalgamated wedge is interpreted as representing a stacking of lobate bodies.

Unit 4

The uppermost sandstone-rich unit at Cerro Divisadero is disrupted by a reverse fault and an increased number of Miocene igneous intrusions, which limit analysis of detailed facies and

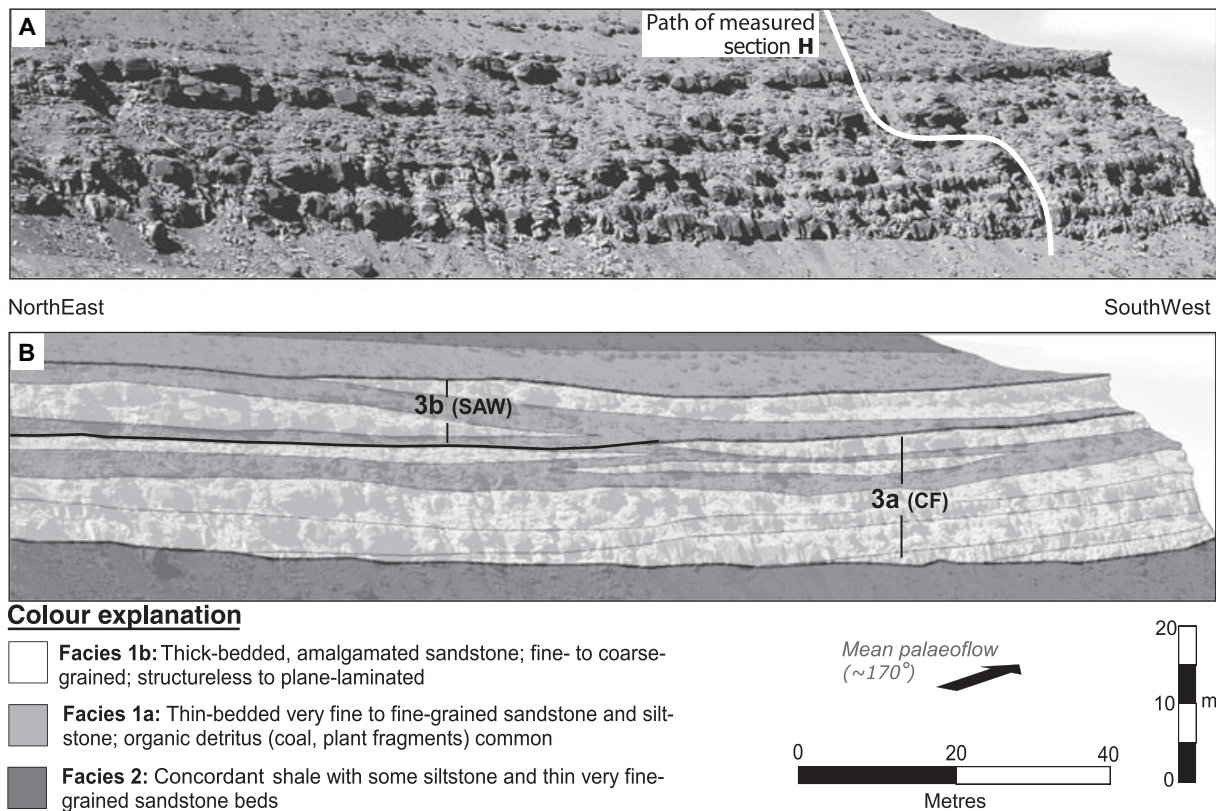


Fig. 16. Photomosaic (A) and interpreted panel (B) of sub-units 3a and 3b. Overlay shows general distribution of F1a and F1b. In this area, the 3a channelform-fill body (CF) is thicker and more sandstone-rich compared to sections to the north (Fig. 15). Note onlapping of lowermost bedsets against basal bounding surface in sub-unit 3a. Palaeocurrents suggest that this part of the outcrop is in a more axial position (Fig. 13). Upper sub-unit 3b is defined as a semi-amalgamated wedge (SAW). In this case, discrete sub-elements of F1b are separated by F1a and compensationally stacked.

sedimentary body architecture as done in lower units. The most conspicuous feature of Unit 4 is an abundance of F1c, the coarsest material observed thus far in all of the Tres Pasos Formation in the region (Shultz *et al.*, 2005). This clast-rich interval is present across the entire study area but varies in thickness significantly from less than 2 m to nearly 18 m thick. The basal surface of this interval exhibits erosional truncation of underlying strata. The sandstone deposits overlying the clast-rich interval are approximately 25 m thick and consist primarily of F1a with a notable abundance of medium-grained plane-laminated sandstone. Stratigraphically above Unit 4, the Tres Pasos Formation is dominated by shale (Figs 1 and 4A). This ~400 m thick interval is exposed on an extensive dip-slope east of the Cerro Divisadero ridge and was not studied in detail.

The clast-rich interval within Unit 4 is interpreted as a zone of bypass. The presence of numerous sedimentation units indicates that

many flows came through this area. Abundant traction structures within individual sedimentation units (S_1 division of Lowe, 1982) indicate a relatively high degree of bypass for individual flows. Additionally, the presence of traction structures precludes an interpretation of a more cohesive debris flow-like depositional process. Evidence for erosion at the base of this interval suggests that it may have channelform geometry but this is difficult to document in detail because of post-depositional disruption.

Summary of Cerro Divisadero stratigraphic evolution

Units 1 to 4 are components of kilometre-scale sandstone-rich slope packages that record progradation and aggradation of the Tres Pasos Formation depositional slope system (Fig. 3). Because the progradational geometry (i.e. mappable clinoforms) is larger than the scale of the outcrop, the sedimentological and architectural criteria

outlined above are the most valuable information leading to this interpretation. Figure 17 summarizes the stratigraphic evolution of the lower Tres Pasos Formation within the context of relative gradient and flow-confinement conditions.

Unit 1 has an abundance of MTDs and interbedded metre-scale sandstone intervals that suggest deposition of lobate bodies in a poorly channelized to unconfined setting. The presence of multiple levels of MTDs indicates that this was a site of accumulation for numerous mass wasting events; this is interpreted as a base of slope setting (Fig. 17).

Unit 2 is interpreted as a proximal lobe complex based largely on the characteristics of the basal amalgamated sheet (sub-unit 2a): (i) high sandstone richness, amalgamation index, and average bed thickness (Table 2); (ii) high proportion of thick-bedded, amalgamated sandstone (F1b) (Figs 10B and 11); (iii) combination of lateral variations in degree of amalgamation and diverging palaeocurrent indicators (Figs 11B and 13A); (iv) low lenticularity index (Table 2); (v) basinward (i.e. southward) decrease in evidence for significant channelization and/or scouring (Fig. 11); and (vi) basinward increase in presence of MTDs directly underlying Unit 2 (Fig. 11). These characteristics indicate that the southern part of the succession reflects relatively less confinement which is interpreted as reflecting a slightly lower gradient. Unit 2 is interpreted as having been deposited on the lower slope to base of slope and within a channel-lobe transition zone (Fig. 17).

The basal part of Unit 3 is interpreted as a lower slope channel-fill complex based on: (i) evidence for erosion and sediment bypass along basal bounding surface (Figs 14 and 15); (ii) onlap of beds/bedsets onto the basal erosional surface and overall pinch out of channel-fill body (Figs 14 to 16); (iii) internal cut-and-fill architecture (Fig. 15); and (iv) high lenticularity index (Table 2). These attributes are characteristic of mixed erosional/depositional channel-fills described in the literature (e.g. Mutti & Normark, 1987; Clark & Pickering, 1996) and reflect increased gradient conditions relative to underlying strata (Fig. 17).

The zone of erosion and net bypass recorded by the interval of clast-rich facies in Unit 4 (Fig. 8) reflects the highest gradient and flow confinement conditions observed in the data set. This unit is interpreted as recording deposition on a middle to lower slope position (Fig. 17).

It is inherently difficult to place outcrops of limited extent on a shelf-to-basin depositional profile. The interpretations of profile position made in the present study are within the context of an idealized slope profile, where gradients are highest on the upper slope and decrease systematically downslope (Rich, 1951; Bates, 1953; Van Siclen, 1958). Modern supply-dominated continental margins exhibit this general slope profile (O'Grady *et al.*, 2000). The vertical pattern at Cerro Divisadero thus reflects the basinward advance of the depositional slope. Stacking patterns at the scale of the sandstone-rich units and sedimentary bodies reflect local and transient variability in accommodation/gradient conditions. At the scale of the >600 m thick succession, however, a stacking pattern recording increased gradient conditions is consistent and robust.

DISCUSSION

Depositional models for prograding slopes

Cyclic packaging of sandstone and shale units within a continental margin-scale slope system such as the lower Tres Pasos Formation can variously be ascribed to dominant allogenic drivers, such as: (i) global eustatic changes (Vail *et al.*, 1984; Vail, 1987; Posamentier *et al.*, 1988); (ii) tectonism (i.e. uplift/subsidence) (Cloetingh *et al.*, 1985; Catuneanu *et al.*, 1998); (iii) autogenic processes, such as slope channel-lobe avulsion (Flood *et al.*, 1991; Pirmez & Flood, 1995); or (iv) more proximal delta-lobe switching (Suter & Berryhill, 1985; Steel *et al.*, 2000). Unfortunately, the regionally homoclinal Tres Pasos Formation outcrop and lack of age control preclude definitive discrimination of drivers for sandstone-mudstone packaging. Nevertheless, excellent outcrop quality encourages comparisons to delta-slope models and permits refinement to those models.

Depositional slopes, by definition, record more sediment accumulation than bypass/erosion over long time intervals. The topset portion of the system (i.e. delta and delta front) is able to advance basinward because of net accumulation on the slope (Scruton, 1960). Mud-rich delta-slope systems commonly exhibit striking sigmoidal clinoform geometries recognizable in seismic reflection profiles of Holocene delta systems (e.g. Cattaneo *et al.*, 2003; Liu *et al.*, 2004; Niedoroda *et al.*, 2005). Systems that deliver varying

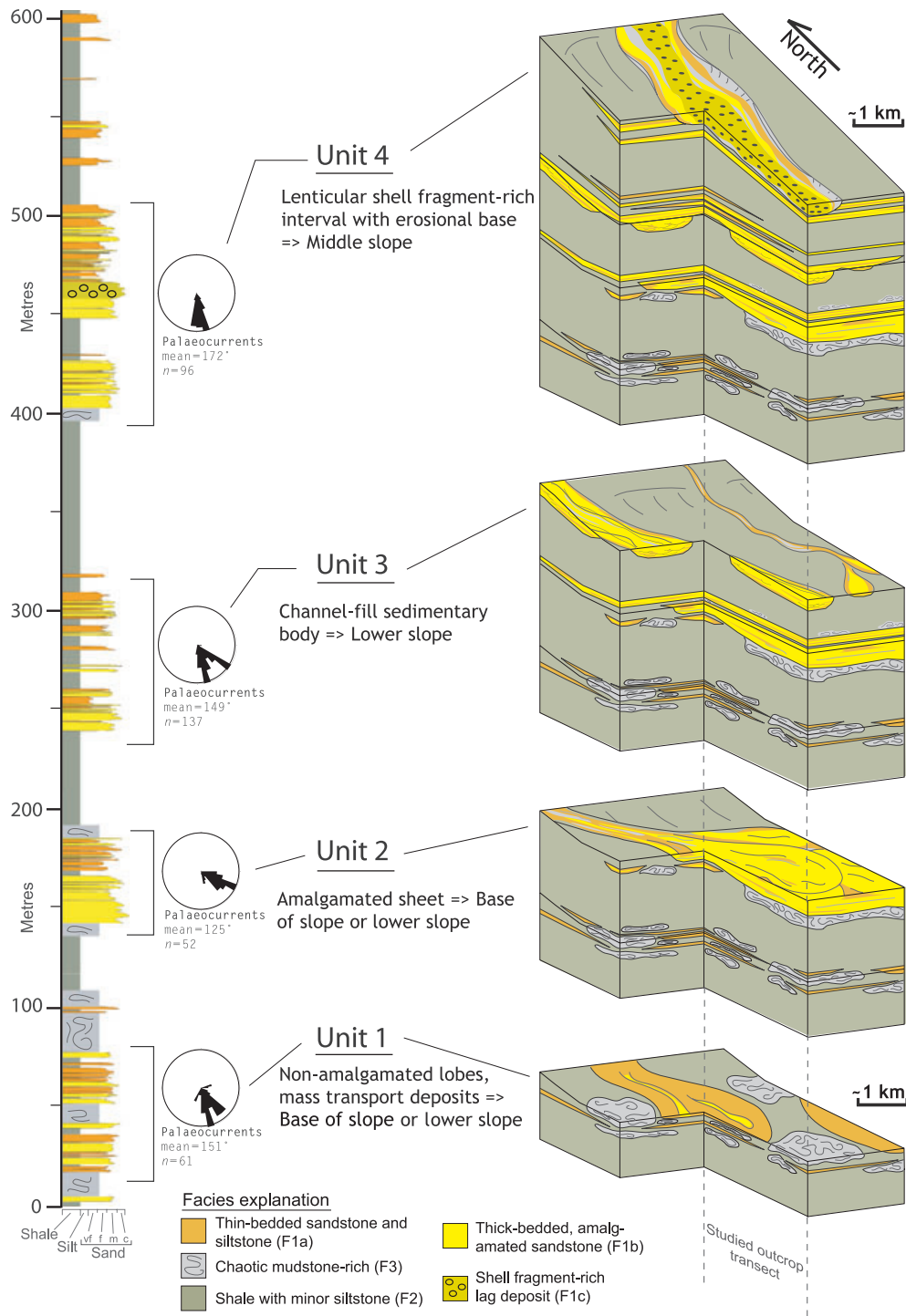


Fig. 17. Type measured section and schematic block diagrams depicting depositional evolution for sandstone-rich Units 1 to 4 in the lower Tres Pasos Formation at Cerro Divisadero. The north–south oriented panel in the cut-away portion of the diagram corresponds to studied outcrop transect showing facies associations. The sedimentology and sedimentary body architecture suggests an overall increase in channellization and flow bypass upward through the succession. Unit 1 is characterized by thin, lobate sandbodies and MTDs at the base of slope. Unit 2 is interpreted as a proximal lobe complex on the lower slope to base of slope. Unit 3 strata record channellization and subsequent back-filling on the lower slope. Unit 4 is characterized by a significant bypass zone that reflects the highest gradients, possibly representing a middle slope position. Collectively, this stacking pattern is interpreted as representing the basinward accretion of the depositional slope system.

Table 2. Summary of metrics for sedimentary body types at Cerro Divisadero.

Stratigraphic unit	Sedimentary body type	Sandstone richness*	Amalgamation ratio†	Lenticularity index‡	Average internal bed thickness (m)§
3e	Non-amalgamated wedge (NAW)	0.56	0.07	0.25	0.11
3d	Semi-amalgamated wedge (SAW)	0.63	0.19	0.17	0.23
3c	Non-amalgamated wedge (NAW)	0.44	0.09	0.30	0.14
3b	Semi-amalgamated wedge (SAW)	0.81	0.33	0.17	0.21
3a	Channel-form-fill (CF)	0.93	0.61	0.27	0.28
2b	Semi-amalgamated wedge (SAW)	0.78	0.38	0.09	0.22
2a	Amalgamated sheet (AS)	0.92	0.57	0.04	0.72

*Total sandstone thickness divided by gross thickness.

†Number of amalgamation surfaces divided by total number of sedimentation units.

‡Lenticularity index is the average change in thickness per 200 m lateral distance divided by the average total thickness of the stratigraphic unit (see text for further explanation).

§Average value determined from all sandstone beds (F1a and F1b) within the interval.

amounts of both mud and sand to the slope, however, generate more complex stratal geometries (e.g. Berg, 1982; Suter & Berryhill, 1985; Sydow & Roberts, 1994) as a result of differing transport processes. Additionally, a broad range of scales of slopes, from smaller delta-front clinoforms to larger-scale packages that onlap proximal parts of the slope, are superimposed on a margin-scale prograding slope system.

The characteristics of the Tres Paso Formation at Cerro Divisadero generally are consistent with attributes of prograding slope models that emphasize sand delivery (e.g. Brown & Fisher, 1977; Chan & Dott, 1983; Heller & Dickinson, 1985; Helland-Hansen, 1992; Galloway, 1998; Steel *et al.*, 2000; Mutti *et al.*, 2003). The majority of Tres Pasos sedimentary bodies are distinct, shale-encased features interpreted as recording mixed erosion and deposition followed by avulsion or abandonment. Sand delivery is punctuated by mass wasting of the slope, reflecting the high mud accumulation rates in high-gradient areas up-system. The lack of thick successions of deposits indicative of mud-rich overbank settings suggests that long-lived aggradational channel-levée systems did not develop. This suggestion is consistent with the notion that slope channels in this setting are relatively short-lived and probably filled soon after creation. High sedimentation rates combined with frequent lateral shifting of feeder systems results in numerous and short-lived slope channels and gullies (Moore & Fullman, 1975). Additionally, slope readjustment processes result in the generation of mud-rich mass wasting deposits and generation of local accommodation that can lead to accumulation of coarse-grained sediment on the

middle to base of slope (Ross *et al.*, 1994; Galloway, 1998). A regional two-dimensional outcrop belt such as the Tres Pasos Formation precludes the ability to confirm the presence of a large-scale and long-lived feeder canyon in areas proximal to Cerro Divisadero but, based on the interpretation of a progradational/aggradational slope, it is inferred that long-lived feeder canyons were not probable.

Interpretation of system progradation in shallow-marine and deltaic strata is based upon the recognition of basinward-stepping stacking patterns of distinct facies tracts that are associated with a specific depositional environment (shoreface, distributary channel, etc.; e.g. Busch, 1971; Van Wagoner *et al.*, 1990). General applicability of a facies tract approach for slope successions based on profile position (e.g. base of slope, middle slope, upper slope) is problematic. Depositional slopes, particularly continental margin-scale examples, commonly have topographically complex profiles that can result in turbidite-system accumulation in various positions along the profile. The interpretation of slope progradation presented here is based on an examination of sedimentological and architectural criteria that reflect relative changes in gradient over significant stratigraphic thickness, rather than a more limiting facies tract or depositional environment approach.

Comparison of Tres Pasos formation to other outcropping slope systems

Continued emphasis on outcrop characterization of deep-water deposits over the past decade has led to increased recognition and appreciation of

depositional slope systems. Although a comprehensive comparative analysis with other slope systems is beyond the scope of this paper, basin-scale characteristics of several well-known outcropping systems are reviewed and compared with the Tres Pasos Formation.

Eocene strata of the Central Tertiary foreland basin of Spitsbergen is among the best-documented and most published examples of an outcropping prograding slope system (e.g. Steel *et al.*, 2000; Plink-Björklund *et al.*, 2001; Mellere *et al.*, 2002; Crabaugh & Steel, 2004; Johannessen & Steel, 2005; Plink-Björklund & Steel, 2005). The shelf-slope systems exposed at Spitsbergen prograded transversely (i.e. perpendicular from trend of fold-thrust belt) into a relatively small piggy-back basin (Blythe & Kleinspehn, 1978). Plink-Björklund & Steel (2005) estimate water depths of 200 to 400 m (not decompact) at the base-of-slope position.

The Carboniferous Gull Island Formation of western Ireland is interpreted as a slope succession overlying basinal turbidites of the Ross Formation in an extensional basin. The Gull Island strata record a complex interfingering of basin-axial transported sandstone-rich turbidites with mudstone-rich MTDs in the lower section which is overlain by a muddy prograding delta-slope in the upper section (Martinsen *et al.*, 2000). The prograding slope succession is interpreted as a distinctly different phase of sedimentation that builds out laterally from the basin margin downlapping onto the older axial basin fill (Martinsen *et al.*, 2003).

The Tanqua depocentre of the Karoo foreland basin, South Africa, has been interpreted as having reached maximum water depths of 500 m (Wickens, 1994; Bouma and Wickens, 1991). More recently, Wild *et al.* (2005) interpreted the upper part of the Skoorsteenberg Formation as a series of stacked channel complexes that accumulated in a lower slope setting of approximately 200 to 300 m water depth.

The Cretaceous Lewis Shale and associated formations of Wyoming record the southward progradation of a shelf-slope–basin system into the subsiding Western Interior Basin during the final regression of the Cretaceous Western Interior Seaway (Pyles & Slatt, 2007). The maximum relief from shelf break to base of slope is interpreted as having been 450 to 500 m (not decompact) (Pyles & Slatt, 2000, 2007; Carvajal & Steel, 2006).

The most important distinction of the Tres Pasos system compared with the slope systems

mentioned above is the scale. Although water depths cannot be determined precisely, bathyal foraminifera from the upper part of the underlying Cerro Toro Formation, interpreted as representing 1000 to 2000 m water depth by Natland *et al.* (1974), and total stratigraphic thickness of the Tres Pasos Formation (>1300 m) suggest water depths of approximately 1000 m (more if compaction is considered). The majority of other outcropping slope systems are from basins on fully continental crust. The quasi-oceanic crustal underpinning of the Magallanes Basin, inherited from the preceding back-arc basin phase, provides additional support for the plausibility of a relatively deep retroarc foreland basin. Additionally, the Tres Pasos slope system prograded parallel to orogenic belt (along the foredeep axis) for at least 70 km (Shultz *et al.*, 2005) reflecting the longitudinal subsidence pattern.

CONCLUSIONS

Outcrops of the lower part of the Tres Pasos Formation at Cerro Divisadero provide an example of a system in which delta-derived mud and sand contributed to the construction and basinward accretion of a continental margin-scale depositional slope. Four sandstone-rich units (20 to 70 m thick) alternate with shale intervals of comparable thickness (40 to 90 m) over a total stratigraphic thickness of >600 m. A hierarchical examination of facies and sedimentary body characteristics of each sandstone unit indicates a systematic upward increase in sediment bypass. The degree of net bypass/deposition is assessed within the context of relative confinement of coarse-grained sediment gravity flows. Lower Units 1 and 2, characterized by poorly channelized to unconfined sand-laden flows and accumulation of mud-rich mass transport deposits, represent base of slope to lower slope settings. Upper Units 3 and 4 exhibit increased evidence of channellization and net bypass indicative of slightly higher gradient positions on the slope. This observation is interpreted as a record of the basinward accretion of the slope system. This information, combined with sub-regional correlations up and down depositional dip, indicates sandstone-rich packages in the order of 10 to 20 km in dip-oriented extent that were deposited in water depths of approximately 1000 m on the lower slope to base of slope. Although outcrops of slope systems of this magnitude are inherently less complete compared with much smaller

outcropping systems, their characterization is essential for understanding processes, stratal architecture and evolution of continental margin-scale slopes.

ACKNOWLEDGEMENTS

Funding for this research was provided by the Stanford Project On Deep-water Depositional Systems (SPODDS), a petroleum industry-funded consortium conducting geological research of ancient and modern turbidite systems throughout the world. Sponsors include Aera Energy, Amerada Hess, Anadarko Petroleum Corp., Chevron, ConocoPhillips, ENI-AGIP, ExxonMobil, Husky Energy, Maersk, Marathon Oil Co., Nexen Energy, Occidental Petroleum, Reliance, RepsolYPF, Rohol-Aufsuchungs A.G. (RAG), and Shell. Field data were collected by the authors with the help of Jacob Covault, Dominic Armitage, and Elizabeth Cassel. Special thanks to Michael Shultz for first visiting these outcrops during his PhD research at Stanford (2000 to 2004). Mike's initial work on these rocks provided motivation, logistical information, and hypotheses to test for this study. This paper benefitted from numerous discussions with many people including Don Lowe, Bill Normark, Jacob Covault, Andrea Fildani, Julian Clark, Dominic Armitage, Bill Morris, Jim Ingle, Tim McHargue, Jon Payne and others. The clarity and focus of this paper was greatly improved by careful reviews from Peter Talling, Vitor Abreu and Ole Martinsen.

REFERENCES

- Adeogba, A.A., McHargue, T.R. and Graham, S.A.** (2005) Transient fan architecture and depositional controls from near-surface 3-D seismic data, Niger Delta continental slope. *AAPG Bull.*, **89**, 627–643.
- Anderson, K.S., Graham, S.A. and Hubbard, S.M.** (2006) Facies, architecture, and origin of a reservoir-scale sand-rich succession within submarine canyon fill: insights from Wagon Caves Rock (Paleocene), Santa Lucia Range, California, U.S.A. *J. Sed. Res.*, **76**, 819–838.
- Arbe, H. A. and Hechem, J. J.** (1985) Estratigrafía y facies de depósitos marinos profundos del Cretácico Superior, Lago Argentino, Provincia de Santa Cruz (Stratigraphy and deep marine deposition facies of the Upper Cretaceous, Lago Argentino, Santa Cruz). *Actas del Congreso Geológico Argentino*, **9**, 7–41.
- Bates, C.C.** (1953) Rational theory of delta formation. *AAPG Bull.*, **37**, 2119–2162.
- Beaubouef, R.T.** (2004) Deep-water leveed-channel complexes of the Cerro Toro Formation, Upper Cretaceous, southern Chile. *AAPG Bull.*, **88**, 1471–1500.
- Berg, O.R.** (1982) Seismic detection and evaluation of delta and turbidite sequences: their application to exploration for the subtle trap. *AAPG Bull.*, **66**, 1271–1288.
- Biddle, K. T., Uliana, M. A., Mitchum, R. M., Jr, Fitzgerald, M. G. and Wright, R. C.** (1986) The stratigraphic and structural evolution of the central and eastern Magallanes Basin, southern South America. In: *Foreland Basins* (Eds P. A. Allen and P. Homewood), pp. 41–63. Int. Assoc. Sed. Spec. Publ., Blackwell, Oxford.
- Blythe, A.E. and Kleinspehn, K.L.** (1978) Tectonically versus climatically driven Cenozoic exhumation of the Eurasian Plate margin, Scabbar; fission track analyses. *Tectonics*, **17**, 621–639.
- Bouma, A.H.** (1962) *Sedimentology of Some Flysch Deposits. A Graphic Approach to Facies Interpretation*. Elsevier, Amsterdam, 168 pp.
- Bouma, A.H. and Wickens, H. de V.** (1991) Permian passive margin submarine fan complex, Karoo Basin, South Africa: Possible model to Gulf of Mexico: Gulf Coast Association of Geological Societies. *Transactions*, **41**, 30–42.
- Brown, L.F., Jr and Fisher, W.L.** (1977) Seismic-stratigraphic interpretation of depositional systems: examples from Brazilian rift and pull-apart basins. *AAPG Mem.*, **26**, 213–248.
- Busch, D.A.** (1971) Genetic units in delta prospecting. *AAPG Bull.*, **55**, 1137–1154.
- Campion, K.M., Sprague, A.R., Mohrig, D., Lovell, R.W., Drzewiecki, P.A., Sullivan, M.D., Ardill, J.A., Jensen, G.N. and Sickafoose, D.K.** (2000) Outcrop expression of confined channel complexes. In: *Deep-Water Reservoirs of the World* (Eds P. Weimer, R.M. Slatt, J. Coleman, N.C. Rosen, H. Nelson, A.H. Bouma, M.J. Styzen and D.T. Lawrence), *Gulf Coast Sec. SEPM Found. 20th Annu. Res. Conf., Houston, TX, 3–6 December 2000*. SEPM CD-ROM Spec. Pub., **28**, 127–150.
- Carvajal, C.R. and Steel, R.J.** (2006) Thick turbidite successions from supply-dominated shelves during sea-level highstand. *Geology*, **34**, 665–668.
- Cattaneo, A., Correggiari, A., Langone, L. and Trincardi, F.** (2003) The late-Holocene Gargano subaqueous delta, Adriatic shelf: sediment pathways and supply fluctuations. *Mar. Geol.*, **193**, 61–91.
- Catuneanu, O., Willis, A.J. and Miall, A.D.** (1998) Temporal significance of sequence boundaries. *Sed. Geol.*, **121**, 157–178.
- Chan, M.A. and Dott, R.H., Jr** (1983) Shelf and deep-sea sedimentation in Eocene forearc basin, western Oregon – fan or non-fan. *AAPG Bull.*, **67**, 2100–2116.
- Chapin, M.A., Davies, P., Gibson, J.L. and Pettingill, H.S.** (1994) Reservoir architecture of turbidite sheet sandstones in laterally extensive outcrops, Ross Formation, western Ireland. In: *Submarine Fans and Turbidite Systems* (Eds P. Weimer, A.H. Bouma and B. Perkins), *Gulf Coast Sec. SEPM Found. 15th Annu. Res. Conf., Houston, TX, 4–7 December 1994*. SEPM Spec. Pub., 53–68.
- Clark, J.D. and Pickering, K.T.** (1996) Architectural elements and growth patterns of submarine channels; application to hydrocarbon exploration. *AAPG Bull.*, **80**, 194–221.
- Cloetingh, S., McQueen, H. and Lambeck, K.** (1985) On a tectonic mechanism for regional sea level variations. *Earth Planet. Sci. Lett.*, **75**, 157–166.
- Crabough, J. and Steel, R.J.** (2004) Basin-floor fans of the Central Tertiary Basin, Spitsbergen: relationship of basin-floor sand bodies to prograding clinoforms in a structurally-active basin. In: *Confined Turbidite Systems* (Eds S. Lomas and P. Joseph), *Geol. Soc. Lond. Spec. Publ.*, **222**, 187–208.

- de Ruig, M.J. and Hubbard, S.M. (2006) Seismic facies and reservoir characteristics of a deep-marine channel belt in the Molasse foreland basin, Puchkirchen Formation, Austria. *AAPG Bull.*, **90**, 735–752.
- Dalziel, I. W. D. (1986) Collision and cordilleran orogenesis: an Andean perspective. In: *Collision Tectonics* (Eds M.P. Coward and A.C. Ries), *Geol. Soc. Lond. Spec. Publ.*, **19**, 389–404.
- Dalziel, I. W. D., De Wit, M. J. and Palmer, K. F. (1974) Fossil marginal basin in the southern Andes. *Nature*, **250**, 291–294.
- Drinkwater, N.J. and Pickering, K.T. (2001) Architectural elements in a high-continuity sand-prone turbidite system, late Precambrian, Kongsfjord Formation, northern Norway; application to hydrocarbon reservoir characterization. *AAPG Bull.*, **85**, 1731–1757.
- Driscoll, N.W. and Karner, G.D. (1999) Three-dimensional quantitative modeling of clinoform development. *Mar. Geol.*, **154**, 383–398.
- Fildani, A. and Hessler, A.M. (2005) Stratigraphic record across a retroarc basin inversion: Rocas Verdes – Magallanes Basin, Patagonian Andes. *Geol. Soc. Am. Bull.*, **117**, 1596–1614.
- Flint, S.S. and Hodgson, D.M. (2005) Submarine slope systems: processes and products. In: *Submarine Slope Systems: Processes and Products* (Eds D.M. Hodgson and S.S. Flint), *Geol. Soc. Lond. Spec. Publ.*, **244**, 27–50.
- Flood, R.D., Manley, P.L., Kowsmann, R.O., Appi, C.J. and Pirmez, C. (1991) Seismic facies and late Quaternary growth of Amazon submarine fan. In: *Seismic Facies and Sedimentary Processes of Submarine Fans and Turbidite Systems* (Eds P. Weimer and M.H. Link). pp. 415–433. Springer-Verlag, New York.
- Fulthorpe, C.S. and Austin, J.A. (1998) Anatomy of rapid margin progradation: Three-dimensional geometries of Miocene clinoforms, New Jersey margin. *AAPG Bull.*, **82**, 251–273.
- Galloway, W.E. (1998) Siliciclastic slope and base-of-slope depositional systems: component facies, stratigraphic architecture, and classification. *AAPG Bull.*, **82**, 569–595.
- Gardner, M.H., Borer, J.M., Melick, J.J., Mavilla, N., Decesne, M. and Wagerle, R.N. (2003) Stratigraphic process-response model for submarine channels and related features from studies of Permian Brushy Canyon outcrops, West Texas. *Mar. Petrol. Geol.*, **20**, 757–787.
- Halpern, M. (1973) Regional geochronology of Chile south of 50° S latitude. *Geol. Soc. Am. Bull.*, **84**, 2407–2422.
- Helland-Hansen, W. (1992) Geometry of facies of Tertiary clinoforms, Spitsbergen. *Sedimentology*, **39**, 1013–1029.
- Heller, P.L. and Dickinson, W.R. (1985) Submarine ramp facies model for delta-fed, sand-rich turbidite systems. *AAPG Bull.*, **69**, 960–976.
- Hickson, T.A. and Lowe, D.R. (2002) Facies architecture of a submarine fan channel-levee complex: the Juniper Ridge Conglomerate, Coalinga, California. *Sedimentology*, **49**, 335–362.
- Hubbard, S.M., Romans, B.W. and Graham, S.A. (2008) Deep-water foreland basin deposits of the Cerro Toro Formation, Magallanes basin, Chile: architectural elements of a sinuous basin axial channel belt. *Sedimentology*, **55**, doi:10.1111/j/1365-3091.2007.00948.
- Johannessen, E.P. and Steel, R.J. (2005) Shelf-margin clinoforms and prediction of deepwater sands. *Basin Res.*, **17**, 521–550.
- Katz, H. R. (1963) Revision of Cretaceous stratigraphy in Patagonian cordillera of Ultima Esperanza, Magallanes Province, Chile. *AAPG Bull.*, **47**, 506–524.
- Liu, J.P., Milliman, J.D., Gao, S. and Peng, C. (2004) Holocene development of the Yellow River's Subaqueous delta, North Yellow Sea. *Mar. Geol.*, **209**, 45–67.
- Lowe, D.R. (1982) Sediment gravity flows: II. Depositional models with special reference to the deposits of high-density turbidity currents. *J. Sed. Petrol.*, **52**, 279–297.
- Macellari, C. E., Barrio, C. A. and Manassero, M. J. (1989) Upper Cretaceous to Paleocene depositional sequences and sandstone petrography of south-western Patagonia (Argentina and Chile). *J. S. Am. Earth Sci.*, **2**, 223–239.
- Manzocchi, T., Walsh, J.J., Tomasso, M., Strand, J., Childs, C. and Haughton, P.D.W. (2007) Static and dynamic connectivity in bed-scale models of faulted and unfaulted turbidites. In: *Structurally Complex Reservoirs* (Eds S.J. Jolley, D. Barr, J.J. Walsh and R.J. Knife), *Geol. Soc. Lond. Spec. Publ.*, **292**, 309–336.
- Martinsen, O.L., Lien, T. and Walker, R.G. (2000) Upper Carboniferous deep water sediments, western Ireland: Analogues for passive margin turbidite plays. In: *Deep-Water Reservoirs of the World* (Eds P. Weimer, R.M. Slatt, J. Coleman, N.C. Rosen, H. Nelson, A.H. Bouma, M.J. Styzen and D.T. Lawrence), *Gulf Coast Sec. SEPM Found. 20th Annu. Res. Conf., Houston, TX, 3–6 December 2000*. SEPM CD-ROM Spec. Pub., **28**, 533–555.
- Martinsen, O.L., Lien, T., Walker, R.G. and Collinson, J.D. (2003) Facies and sequential organization of a mudstone-dominated slope and basin floor succession: the Gull Island Formation, Shannon Basin, Western Ireland. *Mar. Petrol. Geol.*, **20**, 789–807.
- McCaffrey, W.D., Gupta, S. and Brunt, R. (2002) Repeated cycles of submarine channel incision, infill and transition to sheet sandstone development in the Alpine Foreland Basin, SE France. *Sedimentology*, **49**, 623–635.
- Mellere, D., Plink-Björklund, P. and Steel, R.J. (2002) Anatomy of shelf deltas at the edge of a prograding Eocene shelf margin, Spitsbergen. *Sedimentology*, **49**, 1181–1206.
- Miall, A.D. (1985) Architectural-element analysis: a new method of facies analysis applied to fluvial deposits. *Earth-Sci. Rev.*, **22**, 261–308.
- Micael, P.J. (1983) *Emplacement and differentiation of Miocene plutons in the foothills of the southernmost Andes*. PhD thesis, Columbia University, 367 pp.
- Middleton, G.V. and Hampton, M.A. (1973) Sediment gravity flows: mechanics of flow and deposition. In: *Turbidity and Deep Water Sedimentation* (Eds G.V. Middleton and A.H. Bouma), *SEPM, Pacific Section, Short Course Lecture Notes*, 1–38.
- Middleton, G.V. and Hampton, M.A. (1976) Subaqueous sediment transport and deposition by sediment gravity flows. In: *Marine Sediment Transport and Environmental Management* (Eds D.J. Stanley and D.J.P. Swift), pp. 197–218. Wiley, New York.
- Moore, G.T. and Fullman, T.J. (1975) Submarine channel systems and their potential for petroleum localization. In: *Deltas, Models for Exploration* (Ed. M.L. Broussard), Houston Geological Society, 165–189.
- Mutti, E. and Ghibaud, G. (1972) Un esempio di torbiditi di conoide sottomarina esterna: le Arenarie di San Salvatore (Formazione di Bobbio, Miocene) nell' Appennino di Piacenza. *Mem. Acc. Sci. Torino, Classe Sci. Fis., Nat.*, **4**, 40.
- Mutti, E. and Normark, W.R. (1987) Comparing examples of modern and ancient turbidite systems; problems and concepts. In: *Deep Water Clastic Deposits: Models and Case*

- Histories* (Eds J.K. Legget and G.G. Zuffa), pp. 1–38. Graham and Trotman, London.
- Mutti, E. and Normark, W.R.** (1991) An integrated approach to the study of turbidite systems. In: *Seismic Facies and Sedimentary Processes of Submarine Fans and Turbidite Systems* (Eds P. Weimer and M.H. Link), pp. 75–106. Springer-Verlag, New York.
- Mutti, E., Tinterri, R., Benevelli, G., di Biase, D. and Cavanna, G.** (2003) Deltaic, mixed and turbidite sedimentation of ancient foreland basins. *Mar. Petrol. Geol.*, **20**, 733–755.
- Natland, M.L., González, E., Cañón, A. and Ernst, M.** (1974) A system of stages for correlation of Magallanes basin sediments. *GSA Mem.*, **139**, 126.
- Niedoroda, A.W., Reed, C.W., Das, H., Fagherazzi, S., Donoghue, J.F. and Cattaneo, A.** (2005) Analysis of a large-scale depositional clinoformal wedge along the Italian Adriatic coast. *Mar. Geol.*, **222–223**, 179–192.
- O’Grady, D.B., Syvitski, J.P.M., Pratson, L.F. and Sarg, J.F.** (2000) Categorizing the morphologic variability of siliciclastic passive continental margins. *Geology*, **28**, 207–210.
- Pickering, K.T. and Hilton, V.C.** (1998) *Turbidite Systems of SE France: Application to Hydrocarbon Prospectivity*. Vallis Press, London, 229 pp.
- Pickering, K.T., Clark, J.D., Ricci Lucchi, F., Smith, R.D.A., Hiscott, R.N. and Kenyon, N.H.** (1995) Architectural element analysis of turbidite systems, and selected topical problems for sand-prone deep-water systems. In: *Atlas of Deep Water Environments: Architectural Style in Turbidite Systems* (Eds K.T. Pickering, R.N. Hiscott, N.H. Kenyon, F. Ricci Lucchi and R.D.A. Smith), pp. 1–10. Chapman & Hall, London.
- Pirmez, C. and Flood, R.D.** (1995) Morphology and structure of Amazon Channel. In: *Initial Reports of the Ocean Drilling Program* (Eds R.D. Flood, D.J.W. Piper and A. Klaus), College Station, TX, *Ocean Drilling Program*, **155**, 23–45.
- Pirmez, C., Pratson, L.F. and Steckler, M.S.** (1998) Clinoform development by advective diffusion of suspended sediment: modeling and comparison to natural systems. *J. Geophys. Res.*, **103**, 141–157.
- Plink-Björklund, P. and Steel, R.J.** (2005) Deltas on falling-stage and lowstand shelf margins, the Eocene Central Basin of Spitsbergen: Importance of sediment supply. In: *River Deltas; Concepts, Models, and Examples* (Eds L. Giosan and J.P. Bhattacharya), *SEPM Spec. Publ.*, **83**, 179–206.
- Plink-Björklund, P., Mellere, D. and Steel, R.J.** (2001) Turbidite variability and architecture of sand-prone, deep-water slopes: Eocene clinoforms in the Central Basin, Spitsbergen. *J. Sed. Res.*, **71**, 895–912.
- Posamentier, H.W., Jervey, M.T. and Vail, P.R.** (1988) Eustatic controls on clastic deposition I, conceptual framework. In: *Sea-Level Changes: An Integrated Approach* (Eds C.K. Wilgus, B.S. Hastings, C.G. St.C. Kendall, H.W. Posamentier, C.A. Ross and J.C. Van Wagoner), *SEPM Spec. Publ.*, **42**, 109–124.
- Pyles, D.R. and Slatt, R.M.** (2000) A high-frequency sequence stratigraphic framework for the shallow through deep-water deposits of the Lewis Shale and Fox Hills Sandstone, Great Divide and Washakie basins, Wyoming. In: *Deep Water Reservoirs of the World* (Eds P. Weimer, R.M. Slatt, J. Coleman, N.C. Rosen, H. Nelson, A.H. Bouma, M.J. Styzen and D.T. Lawrence), *Gulf Coast SEPM Foundation, 20th Annu. Res. Conf., Houston, TX, 3–6 December 2000*. SEPM CD-ROM Spec. Pub., **28**, 836–861.
- Pyles, D.R. and Slatt, R.M.** (2007) Applications to understanding shelf edge to base-of-slope changes in stratigraphic architecture of prograding basin margins: stratigraphy of the Lewis Shale, Wyoming, USA. In: *Atlas of Deep-Water Outcrops* (Eds T.H. Nilsen, R.D. Shew, G.S. Steffens and J.R.J. Studlick), *AAPG Stud. Geol.*, **56** (CD-ROM), 19.
- Rich, J.L.** (1951) Three critical environments of deposition and criteria for recognition of rocks deposited in each of them. *Geol. Soc. Am. Bull.*, **62**, 1–20.
- Romans, B.W., Shultz, M.R., Hubbard, S.M. and Graham, S.A.** (2007) Facies architecture of slope channel complexes, Tres Pasos Formation at Cerro Divisadero, southern Chile. In: *Atlas of Deep-Water Outcrops* (Eds T.H. Nilsen, R.D. Shew, G.S. Steffens and J.R.J. Studlick), *AAPG Stud. Geol.*, **56**, 132–135.
- Ross, W.C., Halliwell, B.A., May, J.A., Watts, D.E. and Syvitski, J.P.M.** (1994) Slope readjustment; a new model for the development of submarine fans and aprons. *Geology*, **22**, 511–514.
- Scott, K.M.** (1966) Sedimentology and dispersal patterns of a Cretaceous flysch sequence, Patagonian Andes, southern Chile. *AAPG Bull.*, **50**, 72–107.
- Scruton, P.C.** (1960) Delta building and the deltaic sequence – recent sediments, northwest Gulf of Mexico. *AAPG Symp.*, Tulsa, OK, 82–102.
- Shultz, M.R. and Hubbard, S.M.** (2005) Sedimentology, stratigraphic architecture, and ichnology of gravity-flow deposits partially ponded in a growth-fault-controlled slope minibasin, Tres Pasos Formation (Cretaceous), southern Chile. *J. Sed. Res.*, **75**, 440–453.
- Shultz, M.R., Fildani, A., Cope, T.A. and Graham, S.A.** (2005) Deposition and stratigraphic architecture of an outcropping ancient slope system: Tres Pasos Formation, Magallanes Basin, southern Chile. In: *Submarine Slope Systems: Processes and Products* (Eds D.M. Hodgson and S.S. Flint), *Geol. Soc. Lond. Spec. Publ.*, **244**, 27–50.
- Smith, C. H. L.** (1977) *Sedimentology of the Late Cretaceous (Santonian–Maastrichtian) Tres Pasos Formation, Ultima Esperanza District, southern Chile*. Master’s thesis, University of Wisconsin, Madison, WI, 129 pp.
- Steel, R.J., Crabaugh, J., Schellepeper, M., Mellere, D., Plink-Björklund, P., Deibert, J. and Loeseth, T. J.** (2000) Deltas vs. rivers at the shelf edge: their relative contributions to the growth of shelf margins and basin-floor fans (Barremian and Eocene, Spitsbergen). In: *Deepwater Reservoirs of the World* (Ed. P. Weimer), *GCS-SEPM, 20th Annu. Res. Conf., Houston, TX, 3–6 December 2000*. SEPM CD-ROM Spec. Pub., **28**, 981–1009.
- Suter, J.R. and Berryhill, H.L.** (1985) Late Quaternary shelf-margin deltas, northwest Gulf of Mexico. *AAPG Bull.*, **69**, 77–91.
- Sydow, J. and Roberts, H.H.** (1994) Stratigraphic framework of a Late Pleistocene shelf-edge delta, northeast Gulf of Mexico. *AAPG Bull.*, **78**, 1276–1312.
- Vail, P.R.** (1987) Seismic stratigraphy interpretation using sequence stratigraphy, part 1, seismic stratigraphy interpretation procedure. In: *Atlas of Seismic Stratigraphy, v. 1*, (Ed. A.W. Bally), *AAPG Stud. Geol.*, **27**, 1–10.
- Vail, P.R., Hardenbol, J. and Todd, R.G.** (1984) Jurassic unconformities, chronostratigraphy, and sea-level changes from seismic stratigraphy and biostratigraphy. *AAPG Mem.*, **36**, 129–144.
- Van Siclen, D.C.** (1958) Depositional topography – examples and theory. *AAPG Bull.*, **42**, 1897–1913.

- Van Wagoner, J.C., Mitchum, R.M., Campion, K.M. and Rahmanian, V.D.** (1990) Siliciclastic sequence stratigraphy in well logs, cores, and outcrops: concepts of high-resolution correlation of time and facies. *AAPG Methods Explor. Ser.*, **7**, 63.
- Wickens, H. de V.** (1994) *Basin floor fan building turbidites of the Southwestern Karoo Basin, Permian Ecca Group, South Africa*. Ph.D. thesis, University of Port Elizabeth, Port Elizabeth, South Africa, 233 pp.
- Wild, R.J., Hodgson, D.M. and Flint, S.S.** (2005) Architecture and stratigraphic evolution of multiple, vertically-stacked slope channel complexes, Tanqua depocentre, Karoo Basin, South Africa. In: *Submarine Slope Systems: Processes and Products* (Eds D.M. Hodgson and S.S. Flint), *Geol. Soc. Lond. Spec. Publ.*, **244**, 89–111.
- Wilson, T. J.** (1991) Transition from back-arc to foreland basin development in the southernmost Andes: stratigraphic record from the Ultima Esperanza District, Chile. *Geol. Soc. Am. Bull.*, **103**, 98–111.
- Winker, C.D. and Edwards, M.B.** (1983) Unstable progradational clastic shelf margins. In: *The Shelf Break, Critical Interface on Continental Margins* (Eds D.J. Stanley and G.T. Moore), *SEPM Spec. Publ.*, **33**, 139–157.
- Winn, R.D. and Dott, R.H., Jr** (1979) Deep-water fan-channel conglomerates of Late Cretaceous age, southern Chile. *Sedimentology*, **26**, 203–228.
- Wynn, R.B., Kenyon, N.H., Masson, D.G., Stow, D.A.V. and Weaver, P.P.E.** (2002) Characterization and recognition of deep-water channel-lobe transition zones. *AAPG Bull.*, **86**, no. 8, 1441–1462.

Manuscript received 17 July 2007; revision accepted 17 June 2008